AD-A181 703

INVESTIGATION OF THE ELECTRON TRANSPORT PROPERTIES THAT INITIATE SECOND BREAKDOWN

Captain Mark Snyder

April 1987
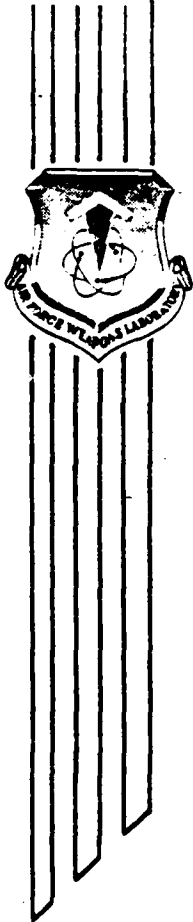
Final Report

Approved for public release; distribution unlimited.

DTIC
ELECTE
JUN 2 4 1987
E

AIR FORCE WEAPONS LABORATORY
Air Force Systems Command
Kirtland Air Force Base, NM   87117-6008

87   6 23 035
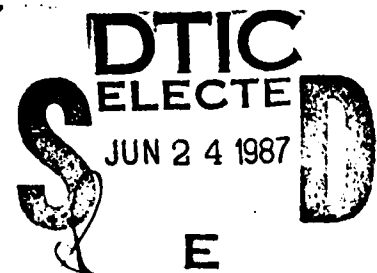
AD-A181 763

REPORT DOCUMENTATION PAGE

1a. REPORT SECURITY CLASSIFICATION Unclassified	1b. RESTRICTIVE MARKINGS
2a. SECURITY CLASSIFICATION AUTHORITY	3. DISTRIBUTION/AVAILABILITY OF REPORT Approved for public release; distribution unlimited.
2b. DECLASSIFICATION/DOWNGRADING SCHEDULE	
4. PERFORMING ORGANIZATION REPORT NUMBER(S) AFWL-TR-85-115	5. MONITORING ORGANIZATION REPORT NUMBER(S)

6a. NAME OF PERFORMING ORGANIZATION Air Force Weapons Laboratory	6b. OFFICE SYMBOL (If applicable) NTA	7a. NAME OF MONITORING ORGANIZATION
6c. ADDRESS (City, State, and ZIP Code) Kirtland Air Force Base, NM 87117-6008		7b. ADDRESS (City, State, and ZIP Code)

8a. NAME OF FUNDING/SPONSORING ORGANIZATION	8b. OFFICE SYMBOL (If applicable)	9. PROCUREMENT INSTRUMENT IDENTIFICATION NUMBER

| 8c. ADDRESS (City, State, and ZIP Code) | 10. SOURCE OF FUNDING NUMBERS |

PROGRAM ELEMENT NO.	PROJECT NO.	TASK NO.	WORK UNIT ACCESSION NO.
64711F	3763	01	55

11. TITLE (Include Security Classification)

INVESTIGATION OF THE ELECTRON TRANSPORT PROPERTIES THAT INITIATE SECOND BREAKDOWN

12. PERSONAL AUTHOR(S)
Capt Mark Snyder

13a. TYPE OF REPORT Final	13b. TIME COVERED FROM 12/83 TO 5/85	14. DATE OF REPORT (Year, Month, Day) 1987, April	15. PAGE COUNT 96

16. SUPPLEMENTARY NOTATION

17. COSATI CODES			18. SUBJECT TERMS (Continue on reverse if necessary and identify by block number)
FIELD	GROUP	SUB-GROUP	Second Breakdown; Failure Mechanisms; Semiconductor
09	02		

19. ABSTRACT (Continue on reverse if necessary and identify by block number)

This paper shows that the phenomenon known as second breakdown is an unstable transition from single-carrier, space-charge-limited current to double-carrier injection. This conclusion is based on B.K. Ridley's analysis showing the transition from single to double carrier injection is inherently unstable on thermodynamic grounds and leads to current filament formation; the primary phenomena associated with second breakdown. Keywords:

20. DISTRIBUTION/AVAILABILITY OF ABSTRACT ☒ UNCLASSIFIED/UNLIMITED ☐ SAME AS RPT. ☐ DTIC USERS	21. ABSTRACT SECURITY CLASSIFICATION Unclassified
22a. NAME OF RESPONSIBLE INDIVIDUAL William R. Ayres	22b. TELEPHONE (Include Area Code) 505-844-9758 22c. OFFICE SYMBOL NTA

DD FORM 1473, 84 MAR

83 APR edition may be used until exhausted.
All other editions are obsolete.

CONTENTS

CONTENTS (Continued)

Accession For

NTIS GRA&I	☒
DTIC TAB	☐
Unannounced	☐
Justification	

By

Distribution/

Availability Codes

Dist	Avail and/or Special
A-1	

DTIC
COPY
INSPECTED
1

ILLUSTRATIONS

ILLUSTRATIONS (Continued)

MODES OF CURRENT CONDUCTION

The electrical characteristics of solids are generally classified as representative of a metal, semiconductor, or insulator.

A metal conducts current in a linear manner characterized by Ohm's Law. Semiconductors and insulators also follow a linear mode of current conduction if the applied electric field is small and the external and internal temperature is moderate (around room temperature). At higher electric fields or extremes of temperature, semiconductors and insulators exhibit nonlinear electrical characteristics representative of the various scattering, generation, and recombination mechanisms involved in the current conduction process. Oftentimes these nonlinear electrical characteristics can give an insulator the low field, moderate temperature characteristics of a semiconductor. Induced nonlinear electrical characteristics can also give a semiconductor the low field, moderate temperature aspects of a metal or an insulator.

Examples of this type of nonlinear behavior are quite common in literature (Refs. 1, 2, and 3). One common example is the ability of lightly doped or pure semiconductors to resemble insulators electrically. At very low temperature at the opposite extreme, semiconductors begin to possess metallic-like values of conductivity (Ref. 1). High temperatures also affect some insulators by increasing their conductivity to an extent. Sometimes, this increase in conductivity is enough to make the insulator resemble a lightly doped semiconductor electrically.

The impression of high electric fields (AC or DC) across semiconductors and insulators can also induce changes in these solids' electrical characteristics. For example, high fields impressed on some insulators can cause permanent or transitory change to the materials electrical characteristics. Although this is accomplished through such mechanisms as breakdown in quartz, other insulators (such as silicon carbide) resemble a semiconductor at high fields near breakdown (Ref. 4). Under high fields, semiconductors can exhibit metallic-like behavior. In particular, this type of behavior is exemplified by the phenomenon called second breakdown (Ref. 5). The phenomenon known as second breakdown is an unstable transition from single-carrier, space-charge-limited current to double-carrier injection.

Alteration of the electrical characteristics of solids can also be attained by chemical means. Doping semiconductors and insulators can make the electrical characteristics appear more metallic. Generally speaking, chemically altering the electrical characteristics of materials is somewhat limited unless augmented by temperature or electrical changes.

This aspect of solids (i.e., the ability to change their electrical characteristics under temperature extremes or changes, high electric fields, or chemical means) demonstrates that the nonlinear aspects of solids can be approximated by a study of their transition from one class of solids to another. In other words, the nonlinear behavior of say, a semiconductor, can be modeled as transitions between semiconductor-like states to metallic- or insulator-like states. This interpretation of nonlinear phenomenon in solids forms the phenomenological basis for the analysis that follows. From it, the importance of space-charge-limited single-carrier currents and double-carrier currents will become obvious in explaining observed nonlinear phenomena. In particular, this provides the basis for explaining the preconditions under which electrically unstable states of operation occur, thus resulting in device transition to second breakdown.

SINGLE-CARRIER CURRENT FLOW

The electrical characteristics of an ideal diode show a high degree of conductivity under forward bias with a small voltage drop across the depletion region. Yet, in reverse bias, the voltage drop across the depletion region is large, giving the impression the depletion region is acting as an insulator. Similar analogies can be demonstrated when carrier transport is explained in terms of current flow through a combination of insulators and semiconductors. These analogies will become clearer upon consideration of single- and double-carrier currents in insulators and semiconductors.

SPACE-CHARGE-LIMITED SINGLE-CARRIER CURRENTS IN INSULATORS

Four situations are examined concerning single-carrier currents in insulators:

1. Perfect trap-free insulator
2. Trap-free insulator with thermal free carriers
3. Trap-filled limit problem
4. Full single-level theory

These treatments are attributable to M.A. Lampert and P. Mark (Ref. 2). The reader can follow the derivations of these treatments in greater depth in Reference 2.

The basic equations used for these various situations are:

$$J = e\mu_n nE + e\mu_p pE \qquad (1)$$

which determines the drift current, but neglects the diffusions current, and Poisson's equation

$$\frac{k\epsilon}{e}\frac{dE}{dx} = [(n - p) + (N_a - N_d)] \qquad (2)$$

PERFECT TRAP-FREE INSULATOR

No thermal free carriers or trap levels are allowed for this situation. The insulator in question possesses ohmic contacts to electrons only. Poisson's equation reduces to

$$\frac{k\epsilon}{e}\frac{dE}{dx} = n \qquad (3)$$

and $J = e\mu_n nE$ combining with $E(x = 0) = 0$ we get

$$\int_0^E E dE = \int_0^x \frac{J}{k\epsilon\mu} dx$$

$$E(x) = \left(\frac{2J}{k\epsilon\mu}\right)^{\frac{1}{2}} x^{\frac{1}{2}}$$

$$V(x) = \int_0^x E \, dx = \left(\frac{8J}{9k\epsilon\mu}\right)^{\frac{1}{2}} x^{\frac{3}{2}} \tag{4}$$

for $x = L$ we get

$$V = V(L) = \left(\frac{8J}{9k\epsilon\mu}\right)^{\frac{1}{2}} L^{\frac{3}{2}}$$

$$J = \frac{9}{8} k\epsilon\mu \left(\frac{V^2}{L^3}\right) \tag{5}$$

known as the trap-free square-law relation.

For the above situation, only electrons carry current, resulting in single-carrier current conduction.

TRAP-FREE INSULATOR WITH THERMAL FREE CARRIERS

Here the problem is complicated by allowing a finite number of thermal carriers to exist without trapping. Poisson's equation becomes

$$\frac{k\epsilon}{e} \frac{dE}{dx} = n - n_0 \tag{6}$$

where n_0 is some finite number of thermally generated electrons. The thermally generated holes do not contribute to current conduction or space charge build-up. Substituting for E, and solving for J we get

$$\frac{k\epsilon}{e} \frac{d}{dx}\left(\frac{J}{e\mu n(x)}\right) = n(x) - n_0$$

$$\frac{k\epsilon J}{\mu e^2} \frac{d}{dx}\left(\frac{1}{n(x)}\right) = n(x) - n_0$$

$$\frac{k\epsilon J}{\mu e^2}\left(\frac{-1}{(n(x))^2}\frac{dn(x)}{dx}\right) = n(x) - n_0$$

$$\frac{-d(n)x}{(n(x))^2} = (n(x) - n_0)\frac{\mu e^2}{k\epsilon J}dx$$

$$-\frac{dn(x)}{(n(x))^3} = \left(1 - \frac{n_0}{n(x)}\right)\frac{\mu e^2}{k\epsilon J}dx$$

$$\frac{-\frac{dn(x)}{(n(x))^3}}{1 - \frac{n_0}{n(x)}} = \frac{\mu e^2}{k\epsilon J}dx$$

multiply both sides by n_0^2

$$\frac{\frac{n_0}{n(x)}\left(\frac{n_0}{(n(x))^3}dn(x)\right)}{1 - \frac{n_0}{n(x)}} = \frac{e^2 n_0^2 \mu}{k\epsilon J}dx$$

let $u = \frac{n_0}{n(x)}$ $w = \frac{e^2 n_0^2 \mu x}{k\epsilon J}$ and $v = \frac{e^3 n_0^3 \mu \cdot V(x)}{k\epsilon J^2}$ and substituting $w_L = \frac{e^2 n_0^2 \mu L}{k\epsilon J}$

in the last equation with $v = \int u dw$ $\frac{udu}{1 - u} = dw$

Integrating, the solution is found to be

with $n = 0$ and $w = 0$ for $E(0) = 0$ $w = -u - ln(1 - u)$

Thus, for all finite w, u is always less than unity so there will always be a finite amount of injected space charge in a solid of finite dimensions. Substituting for u and w in the equation gives

$$J = \frac{e^2 n_0^2 \mu L}{k\epsilon}\frac{1}{w_L}$$

and

$$V = \frac{e n_0 L^2}{k\epsilon}\frac{v_L}{w_L^2} \tag{7}$$

Numerically tabulating w versus u and v versus u, gives Table 1.

5

TABLE 1. Numerical tabulation of w, u, and v.

w	u	1/w	v	u	v/w
8.21	0.9999	0.121	7.71	0.9999	0.114
3.61	0.99	0.277	3.125	0.99	0.239
1.40	0.90	0.714	0.997	0.90	0.508
0.809	0.80	1.23	0.489	0.80	0.747
0.503	0.70	1.988	0.258	0.70	1.01
0.193	0.50	5.18	0.068	0.50	1.82
0.056	0.30	17.85	0.011	0.30	3.50
0.023	0.20	43.47	0.003	0.20	5.67
0.005	0.10	200.0	0.0003	0.10	12.0

The total current is such that J is proportional to 1/w as u varies. The value v is proportional to v/w^2 as u varies. A graph of 1/w versus v/w^2 (Fig. 1) shows an ohmic region and a square law region before space charge limited current flows.

A final quantity of interest here is the distribution of charge in the material. The quantity

$$\frac{n(x) - n_o}{n(l) - n_o} = \frac{w_a(1 - u_a)}{u^2} \tag{8}$$

represents the ratio of the injected charge to the charge at the end of the device. Equation 8 is graphed in Reference 2 and is shown here (Fig. 2). Equation 8 is exact at the extremes of w_a, but is only approximate in between those extremes if the variables are expanded in terms of series.

TRAP-FILLED LIMIT CASE

In this case, the injection level is such that the available traps are all filled. Poisson's equation takes the form

$$\frac{k\epsilon}{e} \left(\frac{dE}{dx} \right) = n(x) + n_t \tag{9}$$

Here, n_t refers to a trapped charge, such as that found in a depletion region of a device. Dimensionless variables similar to the last case are used to solve the following analytic equations:

6
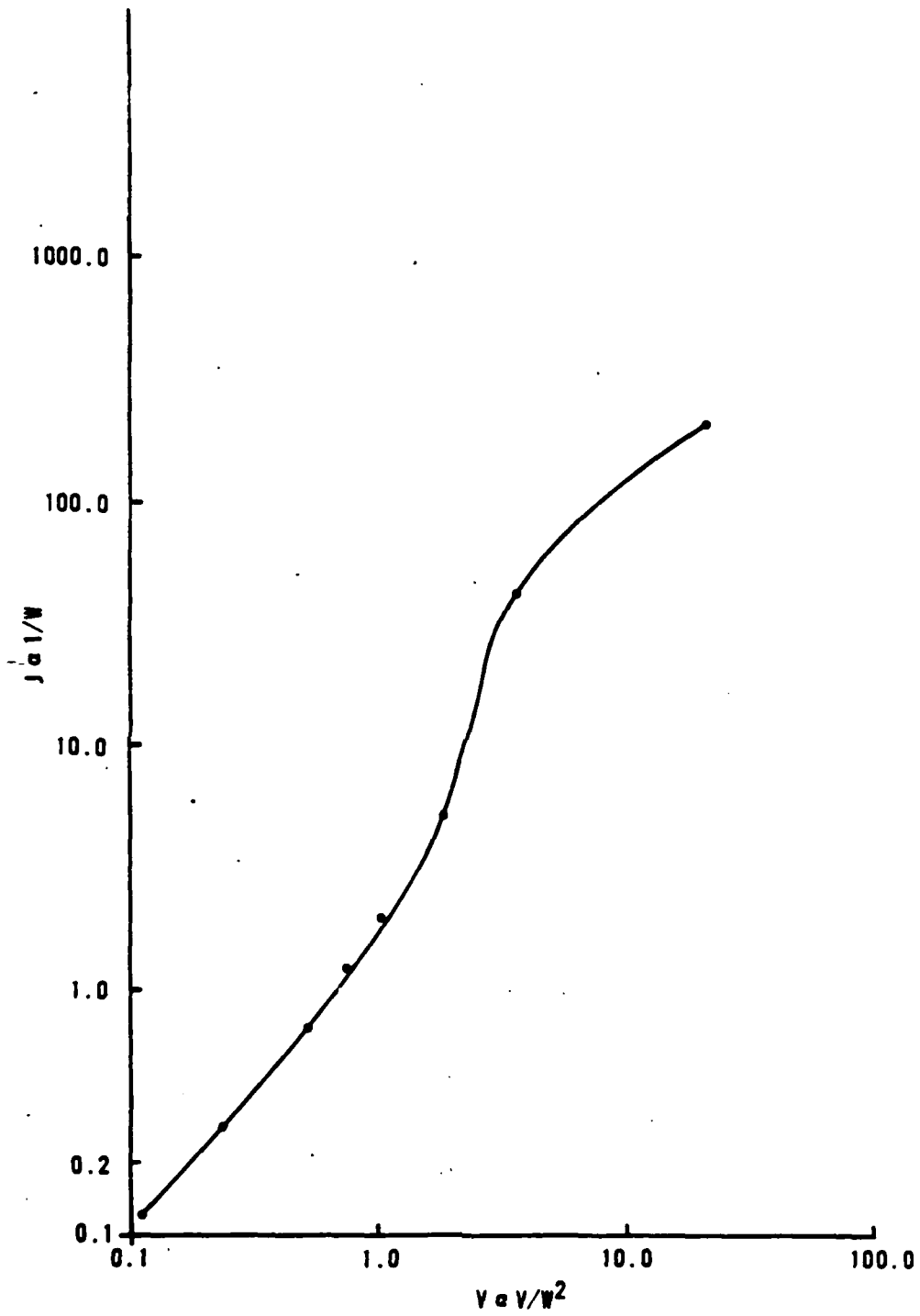
Figure 1. Plot of the dimensionless parts of equation 7.
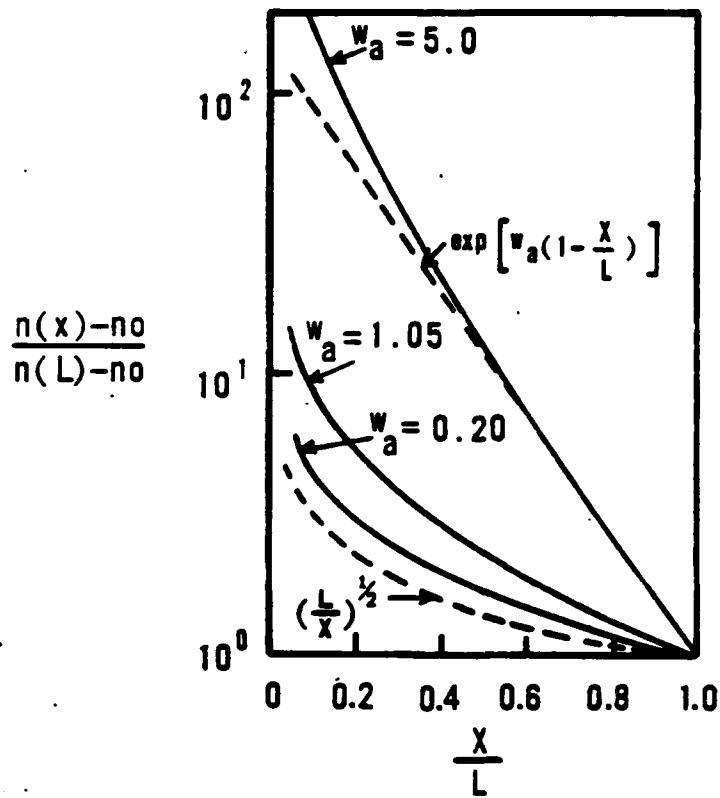
Figure 2. A plot of charge versus length. Note the build-up of spare charge at increasing levels of carrier injection.

$$u_t = \frac{n_t}{\iota(x)} = \frac{en_t\mu_e E(x)}{J}$$

$$w_t = \frac{e^2 n_t^2 \mu_e x}{\epsilon k J}$$

$$v_t = \frac{e^3 n_t^3 \mu_e^2 V(x)}{\epsilon k J^2} \tag{10}$$

Where μ_e is the electrons mobility (independent of e). The differential equation in E becomes

$$\frac{u_t du_t}{1 + u_t} = dw_t$$

the solution is $w_t = u_t - ln(1 + u_t)$

Where $u_t = 0$ at $w_t = 0$ corresponds to E(0) = 0.

The potential is

$$v_t = \int_0^{w_t} u_t dw_t = \frac{1}{2}u_t^2 - u_t + ln(1 + u_t)$$

resulting in

$$J = \frac{e^2 n_t^2 \mu L}{\epsilon k} \frac{1}{w_{ta}}$$

and

$$V = \frac{en_t L^2}{k\epsilon} \frac{v_{ta}}{w_{ta}^2} \tag{11}$$

where the subscript a denotes x = L. Solving for w and v numerically through u, gives the values shown in Table 2.

TABLE 2. Numerical solutions to w and v through known u.

u	w	1/w	v	v/w
0.01	4.9x10	20133	3.3x10	134.11
0.05	1.2x10	826.5	4.0x10	27.44
0.1	4.6x10	213.2	3.1x10	14.1
0.5	9.4x10	10.58	3.04x10	3.40
0.9	0.258	0.387	1.47x10	2.2
0.999	0.306	3.26	1.92x10	2.05
0.99999	0.306	3.25	1.93x10	2.05
1	0.306	3.25	0.193	2.05
5	3.2	0.311	9.29	0.902
10	7.6	0.131	42.39	0.733
50	46	0.021	1203	0.567
100	95	0.01	4904	0.539

The hallmark of the trap-filled limit law is a large change in current over a small change in voltage (Fig. 3).

FULL RECOMBINATION LEVEL THEORY USING THE REGIONAL APPROXIMATION METHOD

An aspect of space-charge-limited current flow that can be used to explain the physical conditions in a semiconductor comes from the monotonically decreasing space charge that naturally occurs in an insulator (Fig. 4).

If the injection level is not high, there will be a plane of x_1 where $n_i(x) = n_0$. This plane will be a function of the level of injected current and will define two regions in the length of the material. One region between 0 and x_1, where $n_i > n_0$ and a second region between x_1 and L where $n_0 > n_i$. Therefore, the simplifying approximation can be made that in Region I (defined as $0 \le x \le x_1$) $n(x) \approx n_i(x)$ and in Region II (defined as $x_1 \le x \le L$) $n(x) \approx n_0$. Thus, this method is called the Regional Approximation. Poisson's equation and appropriate boundary conditions then allow the formulation of solutions in each region showing when transitions to various conduction regimes occur.

This method can be applied to the situation of a set of traps lying in an insulator well above the fermi level by several kT. This situation can be analyzed by constructing a schematic energy band diagram (Fig. 5) that is analogous to the diagram shown in Fig. 4.

This analysis closely follows that of Lampert and Mark (Ref. 2) who have used these methods extensively in analyzing space-charge-limited and double-injection currents.

Region I (defined as $0 \le x \le x_1$) is expressed by the following expressions

$$J = e\mu n E$$

$$\frac{k\epsilon}{e}\left(\frac{dE}{dx}\right) = n$$

$$n(x_i) = N_t$$
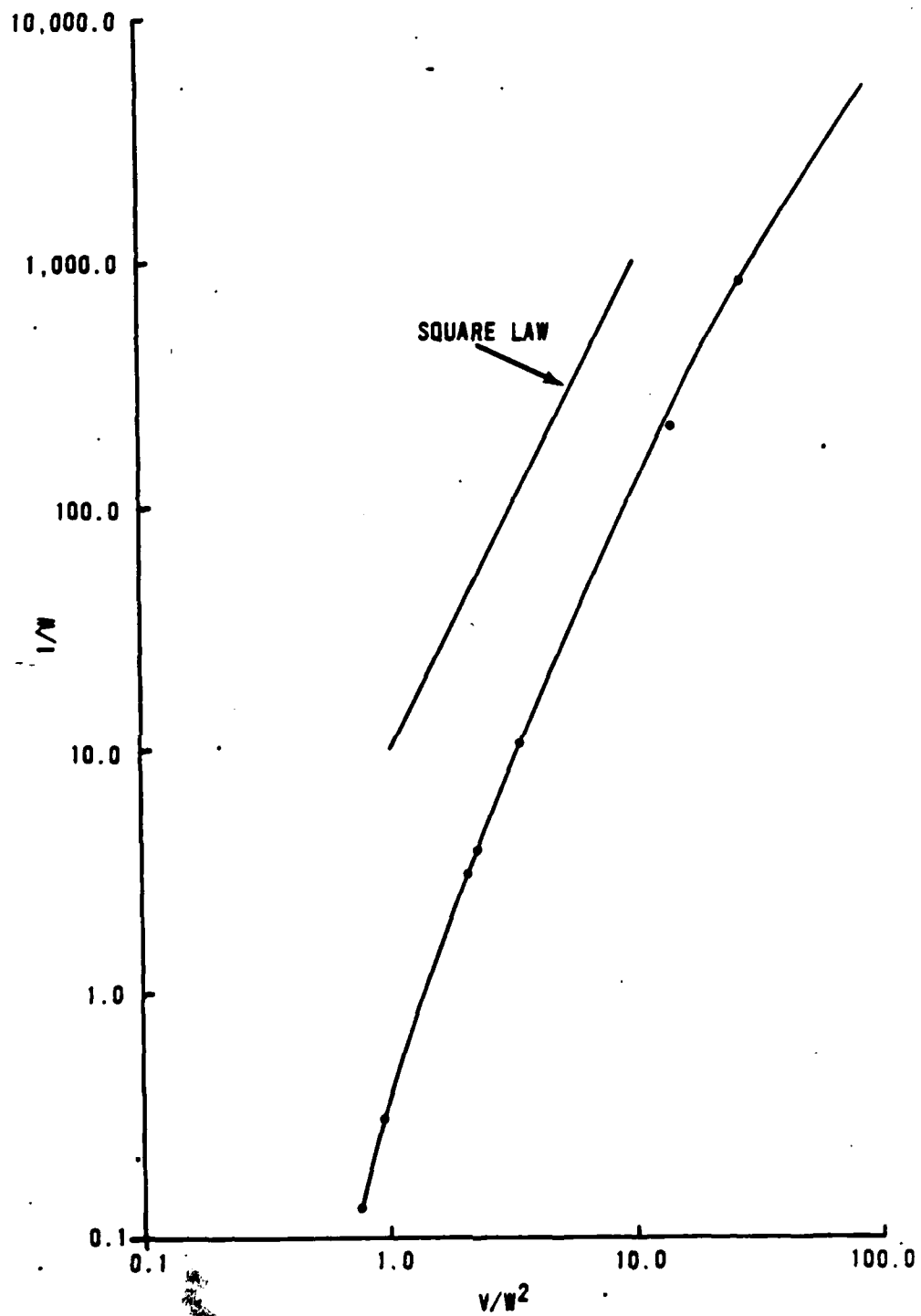
Figure 3.   Dimensionless plot of Table 2.
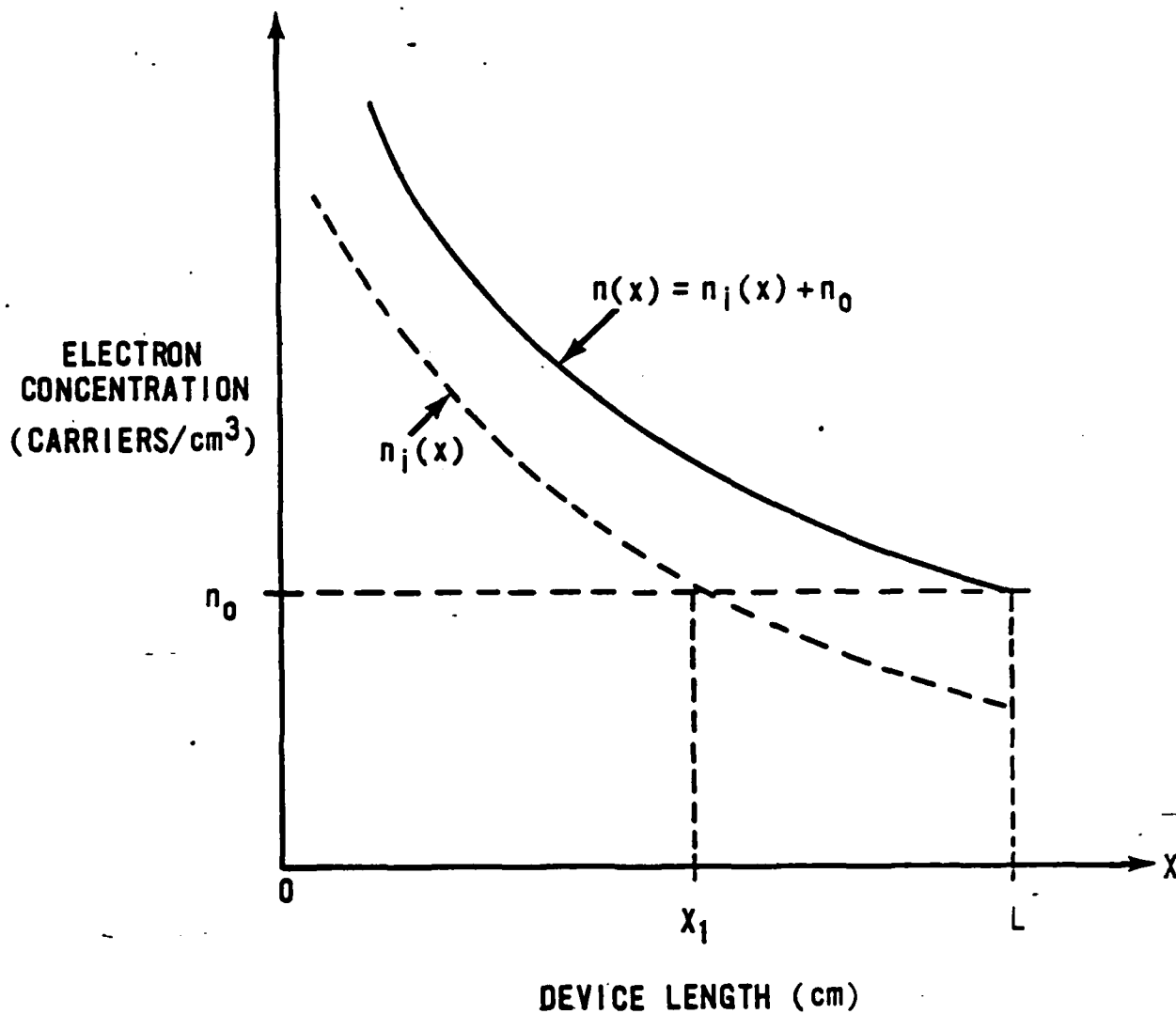
Figure 4. The full off of carrier concentration from the cathode (at x = 0) is similar to full off of carriers from a semiconductor surface illuminated with light. Graph is not to scale.

12
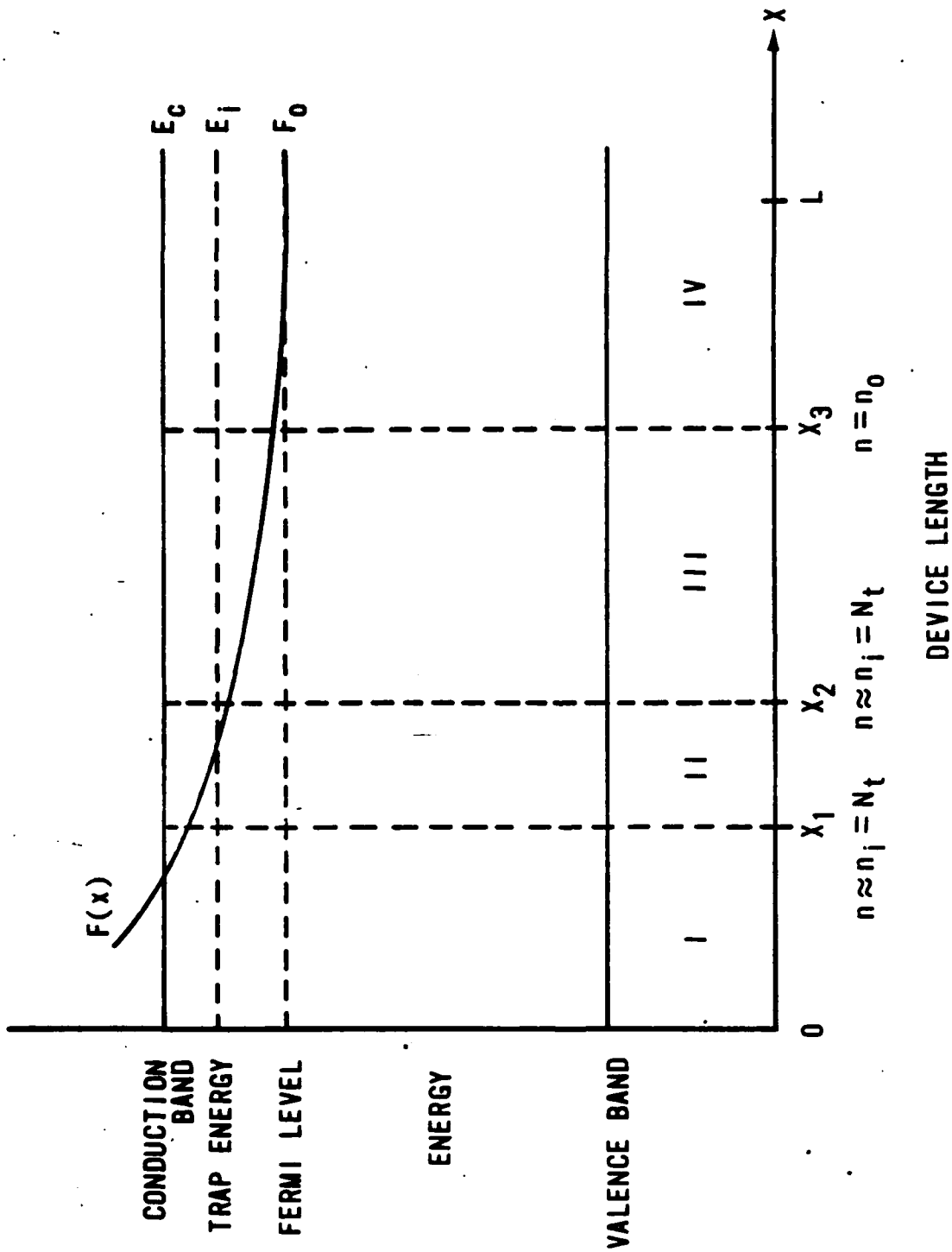
Figure 5. As the carrier concentration decreases across the device F(x) approaches F_0.

13

Region II (defined as $x_1 < x < x_2$)

$$\frac{k\epsilon}{e}\left(\frac{dE}{dx}\right) = N_t$$

$$n(x_2) = \frac{N}{g} = \frac{N_c}{g}\left(\frac{exp(E_t - E_c)}{kt}\right)$$

where

$$n(x) = N_c exp\frac{F(x) - E_i(x)}{kt}$$

$$n_t(x) = \frac{N_t}{1 + 1/g\,(Nn(x))}$$

$$N = N_c exp\frac{(E_t - E_c)}{kt}$$

Here, g stands for the statistical weight for one electronic level to hold one electron. Under certain circumstances, g then takes on such attributes as the thermal ionization rate per unit volume. Under present circumstances the variable will not be identified to a particular mechanism so as to leave the equations general.

Region III (defined as $x_2 < x < x_3$) gives

$$\frac{k\epsilon}{e}\left(\frac{dE}{dx}\right) = \frac{n}{\theta}$$

$$\left(\frac{1}{\theta}\right) = \left(\frac{gN_t}{N}\right)$$

$$\theta \ll 1$$

$$n(x_3) = n_0$$

Region IV (defined as $x_3 < x < L$) gives

$$\frac{k\epsilon}{e}\left(\frac{dE}{dx}\right) = 0$$

It should be noted that Lampert and Mark (Ref. 2) assume that $n \approx N n_t / g N_t$ until $n_t = N_t$. That is, for $n \leq N/g$, $n \quad n_t / g N_t$ and for $n > N/g$, $n_t = N_t$.

By using the dimensionless variables used in the trap-free insulator with thermal carriers, repeated here for clarity, the above Possion's equations can be solved.

$$u = \frac{n_0}{n(x)} = \frac{e n_0 \mu E(x)}{J}$$

$$w = \frac{e^2 n_0^2 \mu x}{k \epsilon J}$$

$$V = \frac{e^3 n_0^3 \mu^2 V(x)}{k \epsilon J^2}$$

For Region I:

$$\frac{du}{dw} = \frac{1}{u} \rightarrow u du = dw \rightarrow u \ = \frac{1}{2} u^2$$

$$v = \int_0^w u dw = \int_0^w u^2 du = \frac{1}{3} u^3$$

$$u_1 = u(w_1) = 1$$

For Region II:

$$\frac{du}{dw} = \frac{N_t}{n_0} \rightarrow \frac{n_0}{N_t} du = dw \rightarrow \frac{n_0}{N_t} u = w$$

$$u = u_1 = 1$$

$$w_1 = \frac{1}{2}$$

For Region III:

$$\frac{du}{dw} = \frac{1}{\theta u} \rightarrow \theta u du = dw \rightarrow \theta \frac{u^2}{2} = w \rightarrow \theta \frac{u^3}{3} \ = v$$

For Region IV:

$$\frac{du}{dw} = 0 \rightarrow u = 1$$

15

Associated with these regions are critical current densities defined so that their appropriate borders (x_1, x_2, and x_3) equal L. Thus, the critical currents are defined as $x_3(J_{cr1}) = L$, $x_2(J_{cr2}) = L$, $x_3(J_{cr3}) = L$. $J < J_{cr1}$ (Ohm's Law regime).

Examination of the boundaries show that for $x_3(J) < L$ all four regions are in the insulator. Yet, calculations show that $\frac{x_1}{x_2} = \frac{N}{2gN_t} \approx \frac{\theta}{2} \ll 1$ and $\frac{x_2}{x_3} = 2(gn_0/N)^2 \ll 1$, since $E_c - F_0 \gg kt$ so Regions I and II contribute negligibly in this regime. Thus, Regions III and IV can be expanded to the cathode. The total potential drop is now

$$V = V_{III} + \left(\int_{w_1}^{w} u\,dw \right)_{IV} = V_{III} + (w - w_1)$$

$$V_a = \frac{\theta}{3} + \left(w_a - \frac{\theta}{2} \right) = \frac{2\theta - 3\theta}{6} + w_a = w_a - \frac{\theta}{6}$$

$$\frac{v_a}{w_a^2} = \left(\frac{1}{w_a} \right) - \frac{\theta}{6} \left(\frac{1}{w_a} \right)^2 \qquad (12)$$

and is the current voltage characteristic. This is Ohm's Law with a small correction term.

This area terminates at a critical current and voltage determined by

$$x_3(J_{cr1}) = L :$$

$$J_{cr1} = \frac{2e^2 n_0^2 \mu L}{\theta \epsilon K}$$

and

$$V_{cr1} = \frac{4en_0 L^2}{3\epsilon k\theta}$$

$$(13)$$

from the before defined dimensionless variables w and v.

The presence of trapping delays the departure from Ohm's Law till a critical current and voltage are reached that is $1/\theta$ times the trap free critical current and voltage.

$J_{cr1} < J < J_{cr2}$ (Shallow-Trap Square-Law Region)

Because $x_3(J) > L$, only Regions I, II, and III are considered. Since the approximation $\frac{x_1}{x_2} \approx \frac{\theta}{2} \ll 1$ is still valid, Region I is again ignored. Region II now extends to the cathode and Region III to the anode. Lampert and Mark (Ref. 2) arrive at

$$\left(\frac{v_a}{w_a} \cdot \frac{n_0^3 g^2}{3 N_t N^2} \cdot \frac{1}{w_a}\right)^2 = \frac{8}{9\theta w_a}\left(1 - \frac{n_0^2 g}{2 N_t N w_a}\right) \tag{14}$$

The shallow-trap square-low current-voltage characteristic terminates at $x_2(J_{cr2}) = L$, so that

$$J_{cr2} = \frac{e^2 n_0^2 \mu L N_t N}{k e n_0^2 g}$$

$$V_{cr2} = \frac{e L^2 N_t}{2kt} \tag{15}$$

where $J_{cr2} < J < J_{cr3}$ (Trap-Filled Limit Region).

Since $x_2(J) > L$, only Regions I and II are considered. This is identical to the trap-filled limit problem already observed; i.e.,

$$\frac{v_a}{w_a^2} = \frac{N_t}{2 n_0} - \frac{n_0}{w_a N_t} - \frac{n_0}{w_a N_t} \ln\left(\frac{n_0}{w_a N_t}\right)$$

$$J_{cr3} = \frac{2 e^2 N_t^2 \mu L}{kt}$$

$$V_{cr3} = \frac{4 e N_t L^2}{3 k\epsilon}$$

where $J_{cr3} < J$ (Trap-Free Square Law Region).

Now only Region I exists, which corresponds to the past case on the trap-free square-law formula.

Figure 6 shows the graph of current versus voltage and the associated regions at current conduction. The regional approximation method thus provides a powerful tool to examine charge injected into a material.
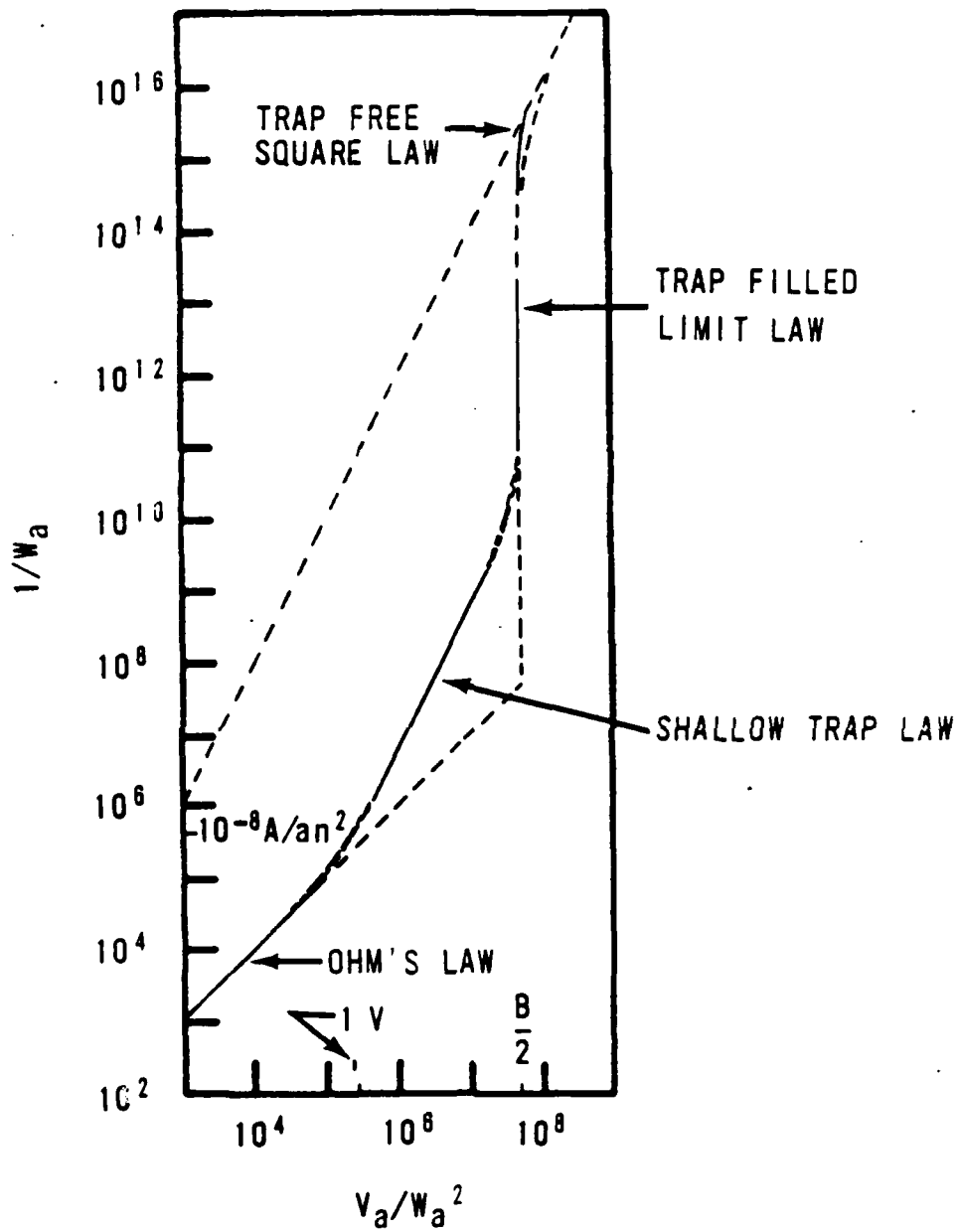
Figure 6. Values used are $\theta = 5 \times 10^{-6}$, $B = 10^8$. Note the transitions from Ohm's Law to the shallow trap law, to the trap filled limit and finally the trap free square law.

18

TWO-CARRIER CURRENTS IN INSULATING MATERIALS

In the previous discussion, single-carrier injected currents were limited by the formation of a space-charge region. If the injecting contacts are allowed to be ohmic for both electrons and holes, space-charge formation is eliminated. Both holes and electrons contribute equally to current flow and the phenomenon called double injection occurs. Since space-charge formation can not occur to limit current flow, a new limiting mechanism appears to provide a limiting regime of current flow; i.e., recombination through localized recombination kinetics.

Recombination can occur via recombination centers that alternate between capturing electrons and holes. Specialized recombination centers (electron and hole traps) may capture only one type of carrier to become neutralized. Such sites will be limited recombination centers whose availability is dependent upon their relative position in the forbidden gap. Direct recombination between valence and conduction band sites will also provide a funnel for carrier recombination. This last mechanism will be directly dependent on the dynamics of carrier injection. Finally, carriers that do not recombine through these various mechanisms can, under low-level injection conditions, recombine directly. The following discussion of recombination takes the simplest approach, that of recombination through recombination sites deliberately placed in the material. The injection level of holes and electrons will also be assumed to be high enough to outnumber the available recombination sites, and approximately neutralize each other at the anode and cathode upon injection into the material being examined.

This situation is referred to in the literature as plasma injection (Ref. 2, p. 210). Discussions in AFWL-TR-85-116 (a companion report) deal more explicitly with the plasma aspects of situation. For now, the expression (plasma injection) will be used as described here.

CONSTANT-LIFETIME PLASMA

Assume that a bar of insulating material, of length L, has a hole injecting anode at $x = 0$, and an electron injecting cathode at $x = L$. The insulator is characterized as possessing a set of recombination centers located several kT above the fermi level at room temperature. The hole capture cross section for this recombination level is much larger than the

electron capture cross section. Thus the electron lifetime is constant for any injection level. A similar situation is expressible for holes with a recombination level below the fermi level. The present discussion will only look at the conditions for constant electron lifetime. The current flow equations are,

$$J_p = e p \mu_p E$$

$$J_n = e n \mu_n E \tag{16}$$

Poisson's equation is

$$\left(\frac{k\epsilon}{e}\right) \frac{dE}{dx} = p - n \tag{17}$$

The conservation equations for the steady state are,

$$\left(\frac{1}{e}\right) \frac{dJ_n}{dx} = \mu_n \left(\frac{d}{dx}\right) nE = r = \frac{n}{\tau_n} = \frac{p}{\tau_p} \tag{18}$$

and

$$-\left(\frac{1}{e}\right) \frac{dJ_p}{dx} = \mu_p \left(\frac{d}{dx}\right) nE = r = \frac{n}{\tau_n} = \frac{p}{\tau_p} \tag{19}$$

Here, τ_n and τ_p are the electron and hole lifetimes, respectively. The assumption here neglects changes in occupancy of recombination centers due to recombination, and hence, constant lifetime for electrons and holes (i.e., the injection level is quite high, far outnumbering the recombination levels in the material). The boundary conditions are the same as before.

Injected--Plasma Regime

In this regime $n \approx p$ everywhere and $\tau_n \approx \tau_p$. The subscripts on the lifetimes are dropped so that the common lifetime is τ. A further assumption is made that τ is independent of injection level or position in the material.

The total current density J is a constant.

$$J = J_n + J_p = e(b+1)\mu_p nE \quad ; \quad b = \frac{\mu_n}{\mu_p} \tag{20}$$

Multiplying Equation 4 by b and adding to Equation 3 gives. using Equations 2 and 5,

$$E\left(\frac{d}{dx}\right)\{E\left(\frac{d}{dx}\right)E\} = -\frac{J}{k\epsilon\mu_p\mu_n r} \tag{21}$$

Elimination of (p-n) is attained by using the Poisson equation. Applying the following dimensionless variables,

$$w = \frac{k\epsilon x}{Jb^{\frac{1}{2}}\mu_p r^2}$$

$$u = \frac{dw}{dy} = \frac{k\epsilon}{e(b+1)\mu_p r_n} = \frac{k\epsilon E}{Jr}$$

$$V = \frac{k^2\epsilon^2 V}{J^2 b^{\frac{1}{2}}\mu_p r^3} \tag{22}$$

where $\bar{v}$ is the applied potential $V(x) = \int_0^x E\,dx$. Substitution of Equation 22 into Equation 21 yields

$$u\left(\frac{d}{dw}\right)\{u\left(\frac{d}{dw}\right)u\} = \frac{d^2u}{dy^2} = -1$$

$$u\left(\frac{d}{dw}\right) = \frac{d}{dy} \tag{23}$$

with the solution

$$u = \frac{1}{2}(y_c y - y^2) \tag{24}$$

where y = 0 at w = w_a = 0 corresponds to $x = 0; y = y_c = y(u_c)$ is the value of y at x = L. Subscripts a and c refer to the anode (x = 0) and cathode (x = L).

Integrating Equation 24 with respect to y yields,

$$w = \int_0^y u\,dy = \frac{1}{4}(y_c y^2 - \frac{2}{3}y^3)$$

$$w_c = \frac{1}{12}y_c^3 \tag{25}$$

Thus, the potential yields,

$$V = \int_0^w u\,dw = \int_0^y \left(\frac{dw}{dy}\right)^2 dy = \frac{1}{12}\left\{ y_c^2 y^3 - \frac{3}{2}y_c y^4 + \frac{3}{5}y^5 \right\} \tag{26}$$

where $v_c = \frac{1}{120}y_c^5$.

In terms of the dimensionless variables,

$$J = \left(\frac{k\epsilon L}{b^{\frac{1}{2}}\mu_p \tau^2}\right)\left(\frac{1}{w_c}\right)$$

and

$$V = V(L) = \left(\frac{L^2}{b^{\frac{1}{2}}\mu_p \tau}\right)\left(\frac{v_c}{w_c^2}\right) \tag{27}$$

Equation 27 shows that J/L is a function of $\frac{V}{L^2}$. Since $\frac{v}{w^3} = 6/5y_c$, it is seen by inspection that

$$\frac{1}{w_c} = \frac{125}{18}\left(\frac{v_c^3}{w_c^2}\right)$$

or that

$$J = \frac{125}{18}\left(k\epsilon\tau\mu_p\mu_n\right)\left(\frac{V^3}{L^5}\right) = \frac{125}{18}k\epsilon\tau\left(\frac{1}{t_p}\right)\left(\frac{1}{t_n}\right)E \tag{28}$$

where τ_p and τ_n are the average transit times for holes and electrons, respectively. As a reminder, it should be noted that this solution for the injected plasma is consistent as long as the transit times for carriers are much smaller than the lifetime. Transit times that approach or are greater than the lifetime result in recombination of carriers before they reach the appropriate contact. This case then results in space-charge limited currents. This situation can be directly related to the voltage applied to the material, since the above situation occurs at relatively high voltages. It appears that a different regime occurs at low voltages.

TRANSITION FROM A ONE-CARRIER SCL CURRENT TO THE INJECTED PLASMA REGIME

Under the initial conditions for the plasma injection regime, it was assumed that the injection level produced more than enough carriers to compensate for the available recombination sites. With n ≈ p under these conditions,

the equations showed that a current density versus the voltage cubed occurred. If the initial conditions are relaxed so that $n \neq p$ anywhere in the insulator, a different situation arises. Again,

$$J = J_n + J_p = e\mu_n nE + e\mu_p pE = constant \tag{29}$$

$$\frac{k\epsilon}{e}\left(\frac{dE}{dx}\right) = p - n \tag{30}$$

The values n and p are separately determined in terms of E and dE/dx. Therefore,

$$(b+1)n = \frac{J}{e\mu_p\epsilon} - \frac{k\epsilon}{e}\frac{d}{dx} \qquad (b+1)p = \frac{J}{e\mu_p\epsilon} + \frac{bk\epsilon}{e}\frac{d}{dx} \tag{31}$$

with $r = n/\tau_n$, multiply by b, and adding to Equation 18 yields,

$$k\epsilon\mu_p\tau_n E\frac{d}{dx}\left\{E\frac{dE}{dx}\right\}k\epsilon E\frac{de}{dx} + \frac{J}{\mu_p} = 0 \tag{32}$$

Using the following dimensionless variables:

$$w = \frac{k\epsilon x}{J\tau_n^2 b\mu_n}$$

$$u = \frac{dw}{dy} = \frac{\epsilon E}{bJ\tau_n}$$

$$v = \frac{k^2\epsilon^2 v}{J^2\tau_n^3 b^2\mu_n} \tag{33}$$

Substitution of Equation 33 into Equation 32 arrives at

$$u\frac{d}{dw}\left\{u\frac{d}{dw}u\right\} - u\frac{d}{dw}u = \frac{d^2u}{dw^2} - \frac{du}{dy} = -1 \tag{34}$$

therefore,

$$u = y - y_c\left\{\frac{(\exp y - 1)}{(\exp y_c - 1)}\right\} \tag{35}$$

where $y = 0$ at $w = w_0 = 0$ for $x = 0; y = y_c = y(w_c)$ for $x = L$.

23

Integration of Equation 35 gives

$$\omega = \int_0^y u\,dy = \frac{1}{2}y^2 + \left\{\frac{y_c}{(\exp y_c - 1)}\right\}(y - \exp y + 1) \tag{36}$$

$$w_c = w(y_c) = \frac{1}{2}y_3^2 - \left(1 - \frac{y_c}{\exp y_c - 1}\right)y_c \tag{37}$$

The potential is:

$$v = \int_0^w u\,dw = \int_0^y \left(\frac{dw}{dy}\right)^2 dy \tag{38}$$

$$v = \left(\frac{y_c}{(\exp y_c - 1)}\right)^2 \left(y - 2(\exp y - 1) + \frac{1}{2}(\exp 2y - 1)\right)$$
$$+ \left(\frac{y_c}{\exp y_c - 1}\right)(y^2 + S(\exp y - 1) - 2(\exp y - 1) - 2y \exp y) + \frac{1}{3}y^3 \tag{39}$$

$$v_c = v(y_c) = \frac{1}{3}y_c^3(\frac{3}{2} - M_c)y_c^2 + (2 - M_c)(1 - M_c)y_c \tag{40}$$

where $M_c = \dfrac{y_c}{\exp y_c - 1}$ This yields,

$$J = \left(\frac{k\epsilon}{\tau_n^2 b \mu_n}\right)\left(\frac{1}{w_c}\right)$$

$$V = V(L) = \frac{L^2}{\mu_n \tau_n}\left(\frac{v_c}{w_c^2}\right) \tag{41}$$

$$\frac{v_c}{w_c^2} = \frac{\frac{2}{3}y_c^3 - (\frac{3}{2} - M_c)y_c^2 + (2 - M_c)(1 - M_c)y_c}{\frac{1}{4}y_c^4 - (1 - M_c)y_c^3 + (1 - M_c)^2 y_c^2} \tag{42}$$

For $y_c \gg 1$ (opposite of the plasma regime case where $y_c \ll 1$) $w_c^2 \approx y_c^4/4$ and $v_c \approx \dfrac{y_c^3}{3}$ so that

$$\frac{v_c}{w_c^2} = \frac{4}{3y_c} \tag{43}$$

Therefore,

$$J = \frac{9k\epsilon\mu_n V^2}{8bL^2} \tag{44}$$

A one carrier type square law relationship holds as long as y_c remains relatively large. As the injection level increases and y_c becomes very small, a cubed law takes hold (Fig. 7).
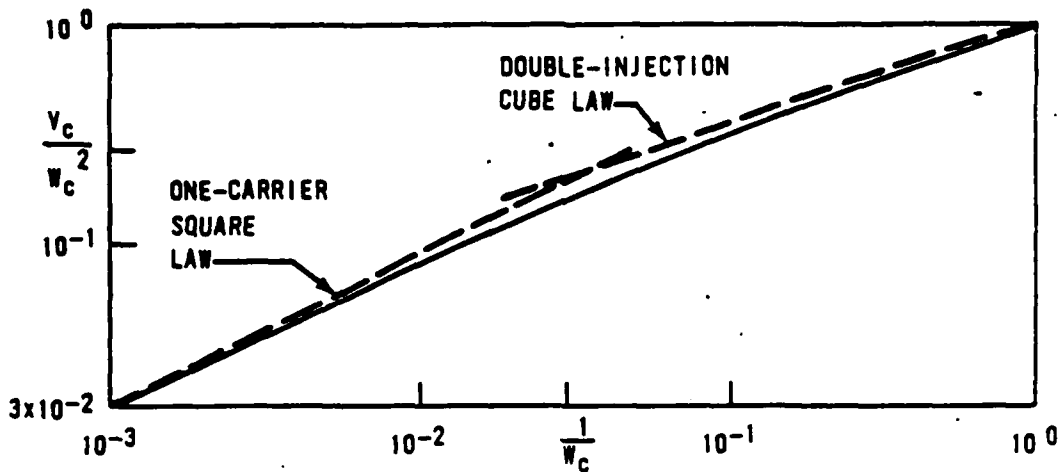
Figure 7. Transition from the one carrier square law to the double injection
cube law in an insulator.

Physically, the mathematics supports the idea that (under the present
assumptions) low field conditions promote the formation of a space-charge-
limited current due to the short lifetime for carriers. As the injection level
increases, enough carriers exist in the material to overcome the ever present
recombination levels to allow double injection.

If the recombination centers are removed from an insulator, injected
electrons and holes will have to recombine directly. This type of plasma is
is known as a bimolecular-recombination plasma. The equations for these
plasma are as before,

$$J_p = e p \mu_p E$$

$$J_n = e n \mu_n E$$

$$\frac{k\epsilon}{e}\left(\frac{dE}{dx}\right) = p - n$$

$$\left(\frac{1}{e}\right)\frac{dJ_n}{dx} = \mu_n\left(\frac{d}{dx}\right)nE = r = \frac{n}{\tau_n} = \frac{p}{\tau_p}$$

$$-\left(\frac{1}{e}\right)\frac{dJ_p}{dx} = \mu_p\left(\frac{d}{dx}\right)nE = r = \frac{n}{\tau_n} = \frac{p}{\tau_p}$$

except r is now defined as $< v\sigma_R > n_p$. Where $\underline{V}$ is the magnitude of the rela-
tive velocity between an electron and hole, σ_R is the recombination cross

section at some velocity, and <> denotes the average of the enclosed quantity. Since the injected plasma are characterized by $p \approx n$, it is possible to replace p by n everywhere in the equations, except where p-n occurs. Initially, the following equations govern recombination:

$$\frac{1}{e}\left(\frac{dJ_n}{dx}\right) = \mu_n\left(\frac{d}{dx}\right)nE = r = < v\sigma_R > n^2 \tag{45}$$

$$\frac{-1}{e}\left(\frac{dJ_p}{dx}\right) = \mu_p\left(\frac{d}{dx}\right)pE = r = < v\sigma_r > n^2 \tag{46}$$

and

$$J = J_n + J_p = e(b+1)\mu_p nE = constant$$

$$b = \frac{\mu_n}{\mu_p}$$

Using Poisson's equation, the current equation yields

$$E^2\frac{d^2E}{dx^2} = -\left\{\frac{4J^2\mu_R}{k^2\epsilon^2 b(b+1)\mu_p^3}\right\} \tag{47}$$

where

$$\mu_R = \frac{k\epsilon < v\sigma_R >}{2e}$$

Using the following dimensionless variables:

$$w = \frac{8e^2\mu_R^{\frac{1}{2}}}{JL^6 k\epsilon\{b(b+1)\mu_p^3\}^{\frac{1}{2}}}x$$

$$u = \frac{2\mu_R}{(b+1)\mu_p L^3 n} = \frac{2e\mu_R}{JL^3}E \tag{48}$$

Substituting Equation 33 into Equation 32 yields

$$u^2\frac{d^2u}{dw^2} = -1 \tag{49}$$

Lampert and Mark (Ref. 2) then employ the dummy variable S so that

$$u = \left(\frac{w_c^2}{2\pi}\right)^{\frac{1}{4}} \exp\left(\frac{-1}{2}S\right)$$

$$w = \left(\frac{w_c}{\pi^{\frac{1}{2}}}\right) \int_{-\infty}^{S} dS \exp(-S^2) \tag{50}$$

So $S = -\infty$ at $\underline{W} = 0$, $\bar{s} = +\infty$ at $w = w_c$ and u vanishes at these limits. The dimensionless variable v is now defined as,

$$\underline{V} = \frac{(2\pi)^{\frac{3}{4}}(k\epsilon)^{\frac{1}{2}}\{b(b+1)\mu_p^3\}^{\frac{1}{4}}}{2J^{\frac{1}{2}}L^{\frac{3}{2}}p^{\frac{1}{4}}} V \tag{51}$$

then

$$\underline{V}(x) = \int_0^x E dx \propto \int_0^w u dw \propto \int_{-\infty}^{+S} u\left(\frac{dw}{ds}\right) ds \propto \int_{-\infty}^{S} u^3 ds \tag{52}$$

$$\underline{V} = V(S) = \int_{-\infty}^{S} dS \exp\left(-\frac{3}{2}J^2\right)$$

$$\underline{V}_c = V(\infty) = \left(\frac{2\pi}{3}\right)^{\frac{1}{2}} \tag{53}$$

finally,

$$J = \left(\frac{9\pi}{8}\right)^{\frac{1}{2}} k\epsilon \left\{\frac{\mu_p \mu_n(\mu_p + \mu_n)}{\mu_R}\right\}^{\frac{1}{2}} \left(\frac{V^2}{L^3}\right) \tag{54}$$

which is a case of the double-injection square-law regime.

27

TWO-CARRIER CURRENTS IN SEMICONDUCTORS

Previously, it was noted that excessive numbers of thermal free carriers was of no concern in insulators. This assumption is completely withdrawn when considering semiconductors. All basic semiconductor theory is based on the concept of thermally excited carriers playing an important part in all current flow problems. Other important variables that affect carrier dynamics are temperature and carrier injection level.

The presence of thermally produced carriers prevent the build-up of any substantial space charge so, for the analysis performed here, local neutrality is assumed to hold.

Under the circumstances for a n-type semiconductor bar with a hole injecting contact at x = 0 and an electron injecting contact at x = L, the current flow equations become

$$J_p = e p \mu_p E - e D_p \left(\frac{dp}{dx} \right)$$

$$V_T = \frac{kT}{e}$$

$$D_p = V_T \mu_p \tag{55}$$

$$J_n = e n \mu_n E + e D_n \left(\frac{dn}{dx} \right)$$

$$D_n = V_T \mu_n \tag{56}$$

Poisson's equation becomes

$$\frac{k\epsilon}{e} \left(\frac{dE}{dx} \right) = (p - p_0) - (n - n_0) \tag{57}$$

where the subscripted carrier concentrations refer to thermal free carriers only. Particle conservation equations are

$$\frac{1}{e} \frac{dJ_n}{dx} = \mu_n \frac{d}{dx}(nE) + \tau V_T \mu_n \frac{d^2 n}{dx^2} = r = \frac{n - n_0}{\tau} = \frac{p - p_0}{\tau} \tag{58}$$

and

$$-\frac{1}{e}\frac{dJ_p}{dx} = -\mu_p\frac{d}{dx}(pE) + rV_T\mu_p\frac{d^2p}{dx^2} = r = \frac{n - n_0}{\tau} = \frac{p - p_0}{\tau} \tag{59}$$

If local neutrality does not hold, then r corresponds to the carrier whose lifetime is most constant with injection level. Also

$$J = J_n + J_p = e\mu_p(p + bn)E + V_T\mu_p\left(\frac{d}{dx}\right)(bn - p) = constant \tag{60}$$

Multiplying Equation 60 by b and adding Equation 58 gives

$$\left(\frac{d}{dx}\right)\{(n - p)E\} + V_T\left\{\frac{d^2(n + p)}{dx}\right\} - \frac{(b + 1)(n - n_0)}{\mu_n\tau} \tag{61}$$

which can be rewritten as

$$\frac{\epsilon V_T}{e}\left(\frac{d^3E}{dx^3}\right) - \frac{e}{k\epsilon}\frac{d}{dx}\left(E\frac{dE}{dx}\right) + (n_0 - p_0)\frac{dE}{dx} + 2V_T\frac{d^2n}{dx^2} = \frac{(b + 1)(n - n_0)}{\mu_n\tau} \tag{62}$$

The first term on the left-hand side (LHS) of Equation 62 can be dropped because of its small size compared to the diffusion term (the last term on the LHS of Equation 62).

Under high level injection conditions $n \approx p \gg n_0$. For a constant lifetime (neglecting diffusion currents), the current density is

$$J = e\mu_p(b + 1)nE = constant \tag{63}$$

and

$$-\frac{e}{k\epsilon}\frac{d}{dx}\left(\frac{EdE}{dx}\right) + (n_0 - p_0)\frac{dE}{dx} + 2V_T\frac{d^2n}{dx^2} = \frac{(b + 1)n}{\mu_n\tau} \tag{64}$$

The first term on the LHS of Equation 64 can be dropped due to its small size in a semiconductor. The boundary conditions are $J_n(0) = 0$ and $J_n(L) = 0$ and give

$$n(0) = \frac{JL^a}{2e\mu_p V_T}$$

and

$$n(L) = \frac{JL_a}{2e\mu_n V_T} \tag{65}$$

Where

$$L_a = \left(\frac{2V_T \mu_n \tau}{b+1}\right)^{\frac{1}{2}}$$

the ambipolar diffusion constant.

Application of the Regional Approximation method to this problem begins with Fig. 8. The second term of Equation 64 approximates the solution in Region I and the third term of Equation 64 approximates the solution in Region II. Call the second term "Term 1," for Region I, and the third term "Term 2," for Region II. That is, in Region I, Term 1 dominates the equation. The solution here is a decaying exponential for $n(x)$ and a growing exponential for $E(x)$. This implies that Term 2 in Region II is doing the opposite of Term 1 in Region I.

In Region II, Term 2 dominates, giving the solution of a monotonically increasing E with increasing x. Since the solution to Regions I and III are the same, there is a plane where E is maximized in Region II and decreases into Region III to satisfy the boundary conditions. Lampert and Mark (Ref. 2) have solved this problem and found that for increasing voltage, a critical voltage is reached where Region II disappears and Regions I and III join. That voltage is

$$V_{cr} \approx V_T \frac{\pi b^{\frac{1}{2}}}{b+1} exp \frac{L}{2L_a} \tag{66}$$

REGION I REGION II REGION III
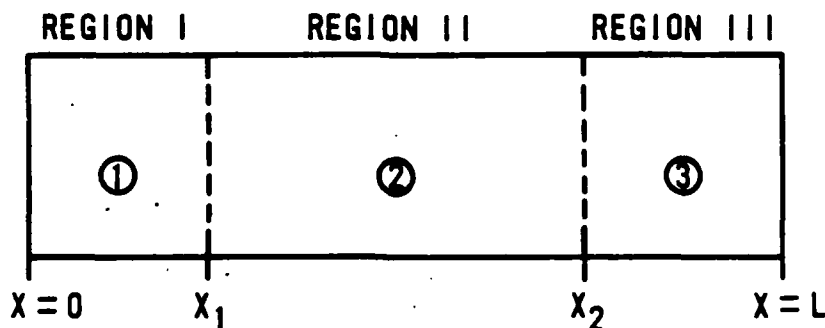
Figure 8. Illustration of the insulator under consideration with depiction of the general regions detailed as regions of differing charge injection.

Beyond this voltage the current increases without further increase in voltage. This conclusion shows that the semiconductor square law holds, but that the length is replaced by an effective spacing L_{eff} so that,

$$J \approx \left(\frac{9}{8}\right) e(n_0 - p_0)\mu_n\mu_p\tau \left(\frac{V^2}{L_{eff}^3}\right) \tag{67}$$

where $L_{eff} = z_2 - z_1$.

For an insulator injected plasma at high injection levels $n = p$ and carrier lifetime is constant. The current equations are

$$J = e\mu_p(b + 1)nE = constant \tag{68}$$

$$-\frac{e}{k\epsilon}\frac{d}{dx}\left(\frac{EdE}{dx}\right) - 2V_T\frac{d^2n}{dx^2} = \frac{(b+1)n}{\mu_n\tau} \tag{69}$$

As in Fig. 8, Regions I and III are dominated by Term 2 while Region II is dominated by Term 1. Lampert and Mark solved this set of equations to find a similar critical voltage as sound in the semiconductor injected plasma problem.

The current was found to follow a cubed law as found with insulators,

$$J \approx \left(\frac{125}{18}\right) \epsilon\mu_p\mu_n\tau \left(\frac{V^3}{L_{eff}^5}\right)$$

$$L_{eff} = z_2 - z_1 \tag{70}$$

For semiconductor devices or materials with heavy doping experiment has found excellent agreement as shown in Fig. 9 (from Ref. 6).

Materials with very light doping, such as the intrinsic region of a PIN device exhibit a cubed law relation as shown in Fig. 10 (from Ref. 7).

The previous discussion lays the basis for studying carrier injection which includes effects due to changes in occupancy of recombination centers or changes in carrier lifetime with an injection level.

This discussion also point out that the depletion region of a device can be modeled as semiconductor or insulator-like regions dependent on the injection level applied to the device.
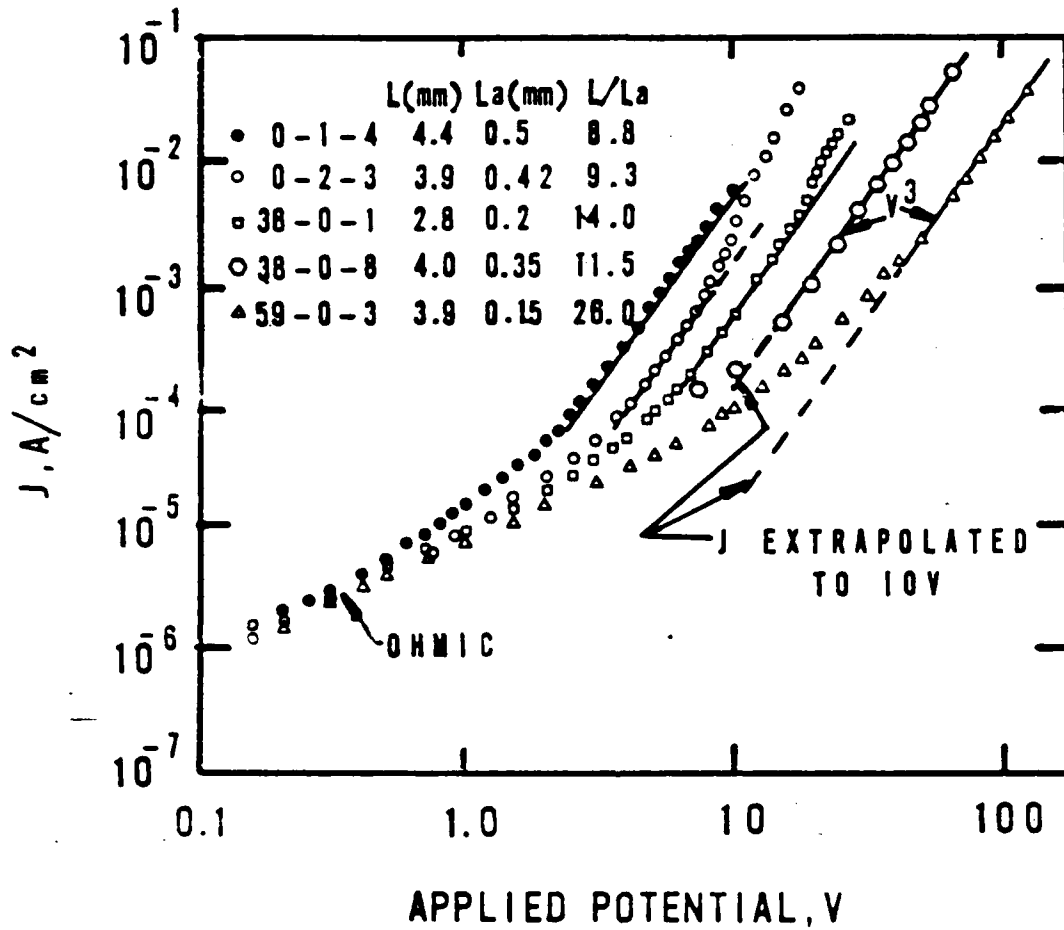
Figure 9. Current density versus reverse voltage at 300 K for PIN junctions whose intrinsic lengths L and ambipolar diffusion lengths L_a are shown. Solid lines are J and V^3 (Ref. 6).

32
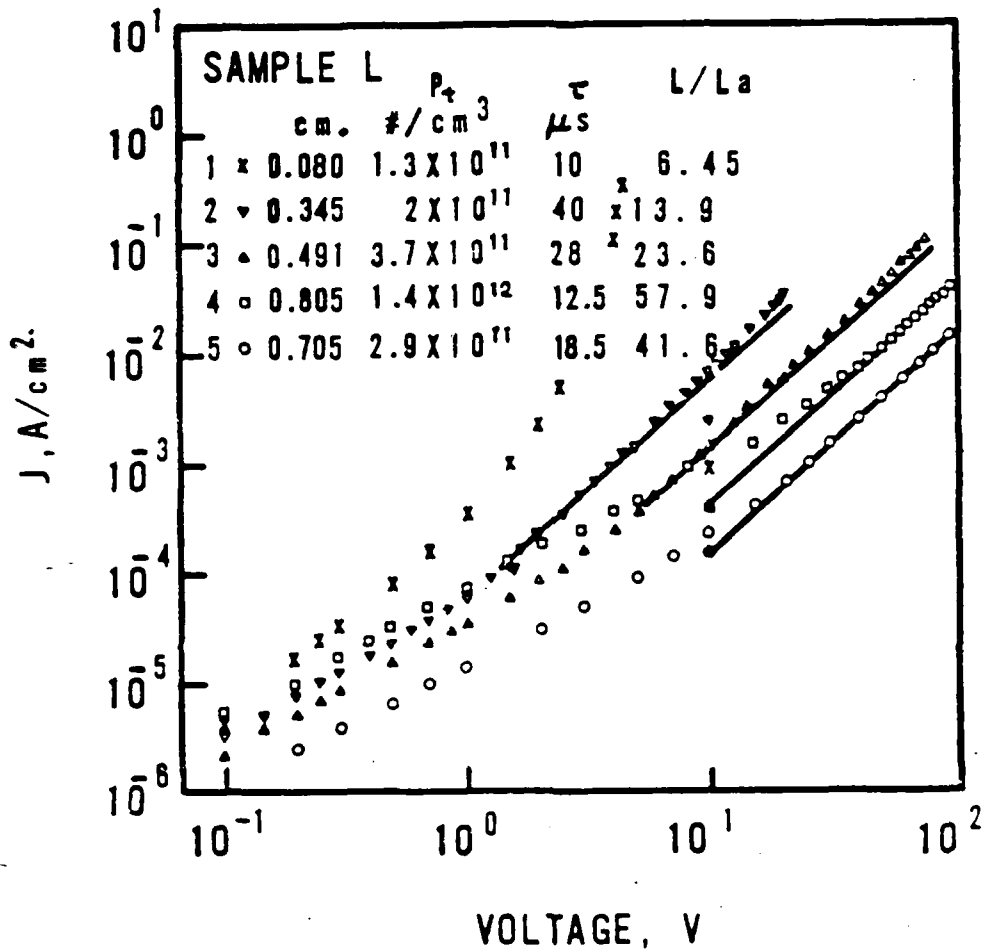
Figure 10. The current voltage characteristics for double injection into lightly doped p-type silicon (Ref. 7).

DOUBLE INJECTION WITH TRAPPING--THE NEGATIVE RESISTANCE CASE

Figures 11 and 12 detail the situations that will be analyzed for recombination centers that are fully occupied in an insulator.

In this situation, the capture cross section for holes is much larger than for electrons (since full acceptor states are involved). The equations governing current flow are

$$J = e\mu_n nE \; + \; e\mu_p pE = constant \tag{71}$$

the local neutrality condition, neglecting space charge is

$$n = p + p_R \tag{72}$$

p_R = concentration of empty acceptor states

$$\mu_n \left(\frac{d}{dx}\right)(nE) = r = -\mu_p \left(\frac{d}{dx}\right)(pE) \tag{73}$$

$$r = \frac{n}{\tau_n} = \frac{p}{\tau_p}$$

$$\frac{1}{\tau_n} = <v\sigma_n> p_R$$

$$\frac{1}{\tau_p} = <v\sigma_p> n_R$$

$$p_R + n_R = N_R \tag{74}$$

Where N_R is the total number of acceptors.

Equation 73 can be rearranged to yield

$$\frac{d}{dx}[(n-p)E] = \frac{(a+1)n}{\mu_p \tau_n} = \frac{(a+1)p}{\mu_p \tau_p}$$

$$a = \frac{\mu_p}{\mu_n} = \frac{1}{b} \tag{75}$$

The boundary conditions are as before, $E = 0$ at $x = 0$. Using the Regional Approximation method, the insulator is divided into two regions: Regions I and II. In Region I, extending from the anode to $x = x_1$, $p(x) > N_R$ and the

CONDUCTION BAND _____ E_C

FERMI LEVEL _____ E_F

ACCEPTOR LEVEL — — — — — — — E_R
_____ E_V
VALENCE BAND
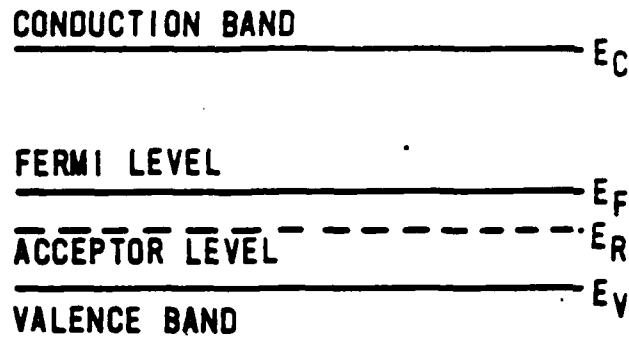
Figure 11. Energy band diagram showing the
relative positions of the acceptor
and Fermi level to the conduction
and valence bands.

```
            I            II          III         IV
            |            |     TRANSITION  FREE
  ANODE  ←─ NUETRALITY HOLDS ─→ REGION ─→ ELECTRON ─→  CATHODE
            |            |            |    REGION
         ←─  n ≈ p  ─→ p << n₁(J ≈ Jn)₁ nR = NR ─→
            |            |            |    |
      X = 0         X₁          X₂          X₃         L
```
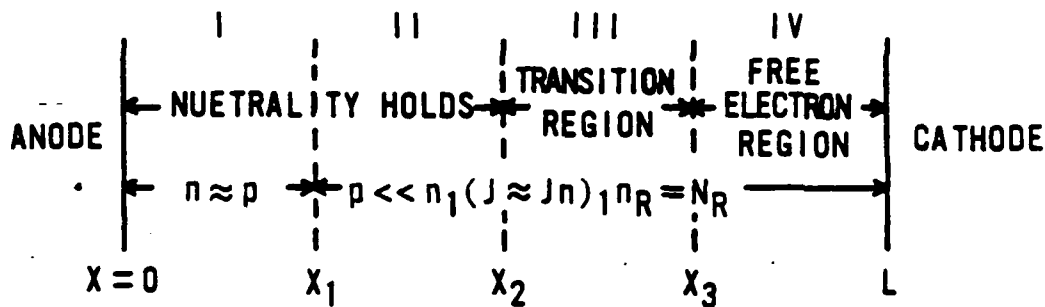
Figure 12. Schematic diagram of the regions and boundary conditions
for the study of double injection with trapping.

recombination centers are mostly unoccupied. Region II, extending from the
cathode to x_1, contains fully occupied recombination centers. In Region I
where $n > N_R$ and $p_R \approx N_R$ in Equation 72, Equation 74 becomes

$$N_R \left(\frac{dE}{dx} \right) = \left[\frac{(a+1)n}{\mu_p \tau_h} \right]$$

$$\left(\frac{1}{\tau_h} \right) = < v\sigma_p > N_R \tag{76}$$

where τ_h is the high injection level lifetime, while Equation 56 evolves to

$$J = e\mu_n E(a+1)n - e\mu_p N_R E \tag{77}$$

35

Substituting $(a + 1)$ in Equation 77 into Equation 76 yields

$$\left[\frac{E}{E + \frac{J}{e\mu_p N_R}}\right] dE = \frac{1}{\mu_n \tau_h} \; dx \tag{78}$$

with the solution

$$E - \frac{J}{e\mu_p N_R} \ln\left[\frac{\left(E + \frac{J}{e\mu_p N_R}\right)}{\frac{J}{e\mu_p N_R}}\right] = \frac{x}{\mu_n \tau_h} \tag{79}$$

solving for the potential drop

$$V(x) = \int_0^x E \, dx = \int_0^E E\left(\frac{dx}{dE}\right) dE$$

$$= \mu_n \tau_h \left(\frac{E^2}{2} - \frac{JE}{e\mu_p N_R} + \left(\frac{J}{e\mu_R N_R}\right)^2 \frac{\ln\left(E + \frac{J}{e\mu_R N_R}\right)}{\frac{J}{e\mu_R N_R}}\right) \tag{80}$$

At the edge of Region I where $x = x_1$

$$n_1 = n(x_1) = N_R$$

$$E_1 = E(x_1) = \frac{J}{e\mu_n N_R} = \frac{aJ}{e\mu_p N_R} = a \, J \tag{81}$$

Substituting Equation 81 into Equations 79 and 80 yields

$$x = \mu_n \tau_p J\{a - \ln(1 + a)\}$$

$$V(x_1) = \mu_n \tau_h J^2 \{\frac{1}{2}a^2 - a + \ln(a + 1)\} \tag{82}$$

Letting J_m and v_m correspond to $x_1 = L$, that is, $n = N_R$ at the cathode, then Equation 82 becomes

$$J_m = \frac{a}{a - \ln(1 + a)} \frac{e N_R L}{\tau_h}$$

$$V_m = \frac{a(\frac{1}{2}a^2 - a + \ln(1 + a)}{(a - \ln(1 + a))^2} \frac{L^2}{\mu_p \tau_h} \tag{83}$$

after application to Equation 78.

In Region II, $n < N_R$, $p \ll n$, $p_R \approx n$, and $n_R \approx N_R$. Applying these constraints to Equation 75 results in

$$p \approx \frac{n^2 < v\sigma_n >}{N_R < v\sigma_p >}$$ (84)

and for the current flow Equation 71

$$\frac{J}{e\mu_n} = nE + \frac{\mu_p}{\mu_n} pE = nE \left(1 + \frac{ap}{n}\right) = nE \left(1 + \frac{a < v\sigma_n > n}{N_R < v\sigma_p >}\right) \approx nE$$ (85)

Here, the last term is much smaller than one via the assumptions for Region II of the material. Rewriting Equation 82 yields

$$-\frac{dn}{n^2} = \frac{eN_R < v\sigma_p >}{aJ} dx$$ (86)

so that

$$\frac{1}{n} = \frac{1}{N_R} + \frac{eN_R < v\sigma_p >}{aJ}(x - x_1)$$ (87)

The field intensity E is now

$$E \approx \frac{J}{e\mu_n} \frac{1}{n} = \frac{J}{e\mu_n N_R} + \frac{N_R < v\sigma_p >}{\mu_p}(x - x_1)$$ (88)

and

$$V_{II} = \int_{x_1}^{L} E dx = \frac{J}{e\mu_n N_R}(L - x_1) + \frac{N_R < v\sigma_p >}{2\mu_p}(L - x_1)^2$$ (89)

Therefore, the entire applied potential $V_I + V_{II}$ is

$$V = V_m \left\{ \left(\frac{J}{J_m}\right)^2 + \frac{a(a - \ln(1 + a))}{\frac{1}{2}a^2 - a + \ln(a + 1)} \left(\frac{J}{J_m}\right) - \left(1 - \frac{J}{J_m}\right) \right\}$$

$$+ \frac{< v\sigma_p > L^2 N_R}{2\mu_p} \left(1 - \frac{J}{J_m}\right)^2$$ (90)

where

$$\frac{<v\sigma_p> L^2 N_R}{2\mu_p} = \frac{L^2}{2\mu_p r_{p_{low}}} = V_{th}$$

Examination of the first coefficient in a, the second term in Equation 90, shows that the coefficient varies from about 3/2 for $a \ll 1$ to 2 for $a \gg 1$. In comparison, the coefficient in a to V_m in Equation 83 decreases from about 3/8 at $a \ll 1$ to 1/9 for $a \gg 1$. Therefore, unless a is very large $V_{th} > V_m$. Equation 90 can then be simplified further to

$$V \approx V_m \left(\frac{J}{J_m}\right)^2 + V_{th} \left(1 - \frac{J}{J_m}\right)^2 \tag{91}$$

This equation demonstrates that as J varies from zero to J_m, V decreases from V_{th} to V_m where V_{th} corresponds to when the average hole transit time is equal to twice the hole low level injection lifetime (Eq. 90). Although this interesting result still requires a physical explanation, we will resolve the problem with space charge for further insight.

By including space charge in this analysis, the neutrality equation used in the previous analysis

$$n = p + p_R \tag{92}$$

must be replaced by

$$\left(\frac{k\epsilon}{e}\right)\left(\frac{dE}{dx}\right) = p + p_R - n \tag{93}$$

in certain regions of the material, Figure 12 is used to facilitate this.

The space charge cannot be neglected beyond x_2, and Poisson's equation takes the form of Equation 93. Hole penetration is negligible beyond x_3 to the cathode and the mobile electron charge dominates the current flow. The electric field increases in strength as x proceeds from the anode or cathode and peaks in the transition region.

In Region III, the following inequalities hold, $p \ll n$, $n \sim p_R$, $p \ll N_R$ and $n_R \sim N_R$. The differential equation for p_R in this region is directly obtained from Equation 86, i.e.,

$$-\frac{dp_R}{p_R^2} = \left(\frac{eN_R <v\sigma_p>}{aJ}\right) dx \tag{94}$$

Integrating Equation 94 gives

$$\frac{1}{p_R(x)} - \frac{1}{p_R(x_2)} = \left(\frac{eN_R < v\sigma_p >}{aJ}\right)(x - x_2) \tag{95}$$

In Region IV, the following inequalities hold: $p \ll p_R \ll N$, $n_R \approx N_R$.

$$J = e\mu_n nE \tag{96}$$

$$n = -\left(\frac{k\epsilon}{e}\right)\frac{dE}{dx} \tag{97}$$

The solution found previously for a space-charge-limited, trap-free current was

$$E(x) = \left(\frac{2J}{e\mu_n}\right)^{\frac{1}{2}}(L-x)^{\frac{1}{2}}$$

and

$$n(x) = \left(\frac{\epsilon J}{2e^2\mu_n}\right)^{\frac{1}{2}}\left[\frac{1}{(L-x)^{\frac{1}{2}}}\right] \tag{98}$$

Mark and Lampert (Ref. 2) then introduce the dimensionless variables of Equations 99 and 100

$$x = x^{++}w$$

$$E = E^{++}u$$

$$V = V^{++}v \tag{99}$$

$$E^{++} = \frac{2aJ}{k\epsilon N_R < v\sigma_p >}$$

$$V^{++} = E^{++}X^{++} = \frac{4a^2\mu_p J^2}{k^2\epsilon^2 N_R{}^3 < v\sigma_p >^3} \tag{100}$$

39

Region I can be solved using the variables of Equation 99 and 100 with Equations 78 and 79.

$$\frac{\cdot \, udu}{u+A} = a\frac{<v\sigma_n>}{<v\sigma_p>}dw$$

$$\frac{J}{E^{++}e\mu_p N_R} = \frac{k\epsilon <v\sigma_p>}{2ea\mu_p} = A$$

$$a\frac{<v\sigma_n>}{<v\sigma_p>} = \frac{X^{-+}}{\mu_n \tau_p E^{++}} = B$$

$$a = \frac{\mu_p}{\mu_n} \qquad\qquad\qquad (101)$$

equivalent to Equation 93. The solution is, like Equation 94

$$u - \frac{J}{E^{++}e\mu_p N_R}\ln\left\{\frac{\left(u+\frac{J}{E^{++}e\mu_p N_R}\right)}{\frac{J}{E^{++}e\mu_p N_R}}\right\} = \frac{wX^{-+}}{\mu_n \tau_p E^{++}} \qquad (102)$$

Solving with the boundary conditions, similar to those used to solve Equation 94 results in

$$w_1 = \left(\frac{A}{B}\right)\{a - \ln(1+a)\}$$

$$u_1 = u(w_1) = aA \qquad\qquad\qquad (103)$$

The dimensionless voltage across Region I is

$$v(w_1) = \left(\frac{A^2}{B}\right)\{\frac{1}{2}a^2 - a + \ln(1+a)\} \qquad\qquad (104)$$

In Region II, Equation 86 becomes, in dimensionless variables,

$$\frac{du}{dw} = 1 \qquad\qquad\qquad\qquad (105)$$

with the solution $u - u_1 = w - w_1$, from Equation 103.

Also, the plane x_2 in Region II was chosen so that

$$\left(\frac{k\epsilon}{e}\right)\left(\frac{dE}{dx}\right)_2 \approx p_{R.2} \approx n_{R.2} \qquad\qquad (106)$$

which corresponds to

$$u_2 = \left(\frac{JX^{++}}{k\epsilon\mu_n E^{++2}} \right) = \frac{1}{2}$$

$$w_3 = \frac{1}{2} - aA + \left(\frac{A}{B} \right) \{ a - \ln (1 + a) \} \tag{107}$$

$$v_{1.2} = \int\limits_{w_1}^{w_2} u \, dw = \int\limits_{u_1}^{u_2} u \, du = \frac{1}{2}(u_2^2 - u_1^2) = \frac{1}{2} \left(\frac{1}{4} - a^2 A^2 \right) \tag{108}$$

To evaluate Equation 95 at $x = x_3$, fix p_{R_3} to be

$$p_{R.3} = p_R(x_3) = \frac{1}{2} n(x_3) = -\frac{1}{2} \left(\frac{k\epsilon}{e} \right) \left(\frac{dE}{dx} \right)_3 \tag{109}$$

since

$$p_{R.2} = p_R(x_2) = \frac{1}{2} n(x_2) = -\frac{1}{2} \left(\frac{k\epsilon}{e} \right) \left(\frac{dE}{dx} \right)_3 \tag{110}$$

is used to fix x_2. Equation 95, in terms of the dimensionless units becomes

$$\frac{1}{-\frac{1}{2} \left(\frac{du}{dw} \right)_3} - \frac{1}{\left(\frac{du}{dw} \right)_2} = 2(w_3 - w_2)$$

or

$$4(w_r - w_3)^{\frac{1}{2}} = 1 + 2(w_3 - w_2) \tag{111}$$

To approximate $u(E)$ in Region III an interpolation scheme is used. Let $u = U_2(w)$ be the equation for the tangent to the curve $u = u(w)$ in Region II at $w = w_2$. Let $u = U_3(w)$ be the tangent to the curve $u = u(w)$ in Region IV at $w = w_3$. Then

$$u_2(w) = u_2 + (w - w_2) \left(\frac{du}{dw} \right)_2 = u_2 + (w - w_2) \tag{112}$$

and

$$u_3(w) = u_3 + (w - w_3) \left(\frac{du}{dw} \right)_3 = u_3 - \left[\frac{w - w}{(w_r - w_3)^{\frac{1}{2}}} \right] \tag{113}$$

41

Note that

$$\frac{du^2}{dw} = -1 \qquad (114)$$

so that

$$u = (w_c - w)^{\frac{1}{2}}$$

and

$$\frac{du}{dw} = -\frac{1}{2}(w_c - w)^{\frac{1}{2}}$$

for the boundary condition $u_c = u(w_c) = 0$ at $E(L) = 0$.

The voltage applied to Region IV is

$$v_{3,c} = \int_{w_3}^{w} u\,dw = \frac{2}{3}(w_c - w_3)^{\frac{3}{2}} \qquad (115)$$

By using Equation 100 we have the relations determining the current-voltage relationship can be determined. They are

$$\frac{1}{w_c} = \frac{2a\mu_p J}{k\epsilon N_R^2 < v\sigma_p >^2 L}$$

$$\frac{v_c}{w_c^2} = \frac{\mu_p V}{N_R < v\sigma_p >^2 L^2} \qquad (116)$$

Lampert and Mark (Ref. 2) solve these equations in terms of W and V to be

$$\frac{1}{w_c} = \frac{1}{-1 - aA - \left(\frac{A}{B}\right)\{(a - \ln(1+a)) - 1)\} + (y+1)^2|} \qquad (117)$$

$$\frac{v_c}{w_c^2} = \frac{\frac{1}{2}\left(\frac{1}{4} - a^2A^2\right) + \left(\frac{A^2}{B}\right)\{\frac{1}{2}a^2 - a + \ln(1+a)\} + \frac{2}{3}y^3 + \frac{5}{3}y^2 + \frac{1}{4}y - \frac{1}{4} + \left(\frac{1}{48y}\right)}{[-1 - aA + \left(\frac{A}{B}\right)\{(a - \ln(1+a)) + 1)\} + (y+1)^2]^2} \qquad (118)$$

Where $y = (w_c - w_3)^{\frac{1}{2}}$ and $V_c = V_{a,1} + V_{1,2} + V_{2,3} + V_{3,c}$, substitution in Equation 93 then yields

$$\left(\frac{1}{w_c}\right)_m = \frac{h(a)b}{aA}$$

and

$$\left(\frac{v_c}{w_c^2}\right)_m = \frac{B}{ag(a)} \qquad (119)$$

where

$$a = \frac{\mu_p}{\mu_n}$$

$$A = \frac{k\epsilon <v\sigma_p>}{2ea\mu_p} = \frac{J}{e\mu_p N_R E^{++}}$$

$$B = a\frac{<v\sigma_n>}{<v\sigma_p>} = \frac{X^{++}}{\mu_p \tau_p E^{++}}$$

$$h(a) = \frac{a}{a - \ln(1+a)}$$

$$g(a) = \frac{\{a - \ln(1+a)\}^2}{a\{\frac{1}{2}^2 - a + \ln(1+a)\}}$$

This allows the equation (Eq. 91) for the neutrality based characteristic to be written as

$$\frac{V}{V_m} = \left(\frac{J}{J_m}\right)^2 + h(a)\frac{J}{J_m}\left(1 - \frac{J}{J_m}\right) + \frac{ag(a)}{2B}\left(1 - \frac{J}{J_m}\right)^2 \tag{120}$$

The space-charge-based J-V characteristics are compared in Fig. 13 to the neutrality-based J-V characteristics for two sets of material parameters in silicon. The lower set of curves correspond to k = 12,

$$\mu_n = \mu_p = 10^4 \frac{cm^2}{V-s}$$

$$N_R = 10^{15} cm^{-3}$$

$$<v\sigma_R> = 9 \times 10^{-10} cm^3/s$$

and

$$<v\sigma_p> = 3 \times 10^{-6} cm^3/s$$

These values are for silicon near liquid nitrogen temperature. The dimension-less variables correspond to a = 1, A = 10^{-3} and B = 3 X 10^{-4}. The upper set of curves correspond to A = 3 X 10^{-4} and B = 10^{-3}. These situations show that a change in carrier lifetimes, $\tau = \frac{1}{<v\sigma> N_R}$, directly determines when the negative resistance regime will occur. This can even be brought about by a change in material temperature affecting N_R or $<v\sigma>$.
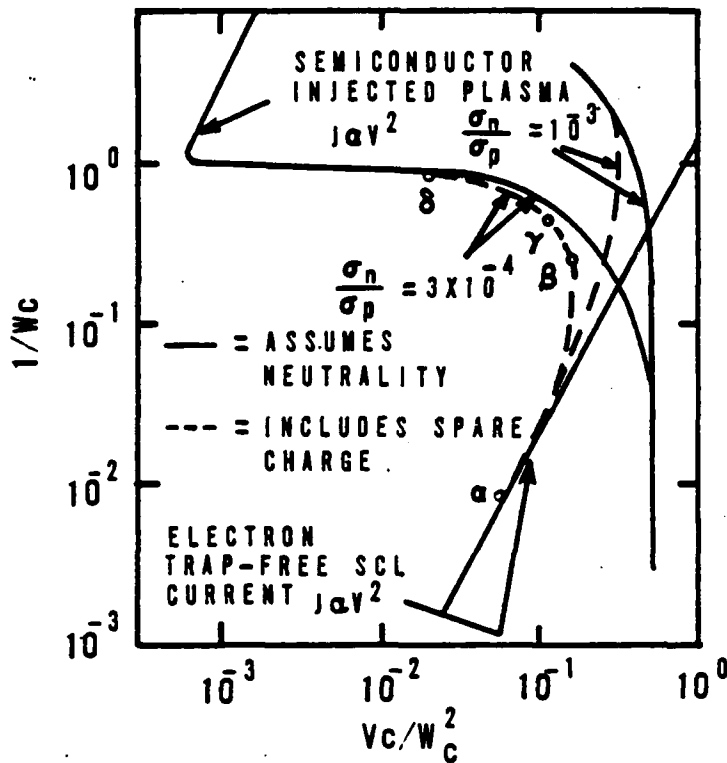
Figure 13. Current density versus voltage for
the case of double injection in an
insulator.

Examination of the four regions assumed for this material as the lower
J-V curve is followed also shows some interesting aspects. At α on the lower
curve, Region IV occupies 83 percent of the material and 81 percent of the
applied voltage. Region III takes the remaining 16 percent of the material and
18 percent of the voltage. Regions I and II take up less than one percent of
the material and voltage. At point β, Regions I and II take up 32 percent of
the material and about two percent of the voltage. Region III takes 43 percent
of the material and 72 percent of the voltage, Region IV takes 25 percent of
the material and about 26 percent of the voltage. At γ, Regions I and II pos-
sess 55 percent of the material but only five percent of the voltage compared
to Region III: 34 percent of the material and 80 percent of the voltage,
Region IV 11 percent of the material and five percent of the voltage. So far
Region IV is continuously shrinking in size. At δ, Region I and II occupy 99
percent of the material and 98 percent of the voltage, Region IV is negligible

and Region III takes the residual. The material moved from a space charge limited current flow to one of plasma injection, demonstrating the theoretical existence of a negative resistance regime. As double injection occurs an electrically unstable situation develops and the material moves to a more stable state as the J-V curve breaks over into current controlled negative resistance.

RECOMBINATION CENTERS PARTIALLY OCCUPIED

In contrast to the previous problem, the recombination centers in this case are allowed to be only partially occupied. This can be accomplished by placing the recombination centers near the Fermi level and assuming that the number of free carriers are negligible, i.e., the centers are primarily defect centers or charged traps.

Once again, the capture cross section for holes is assumed to be much larger than the capture cross section for electrons. As a result, many of the same characteristics seen in the previous problem will occur here.

The basic difference in this problem is the occurrence of a recombination barrier to current flow. In the previous situation, only one carrier type saw any obstruction to current flow. Under present conditions both electrons and holes see a voltage barrier that must be overcome before current can flow (Fig. 14).

CONDUCTION BAND
E_C

FERMI LEVEL
E_F

E_R
TRAP LEVEL

E_V
VALENCE BAND
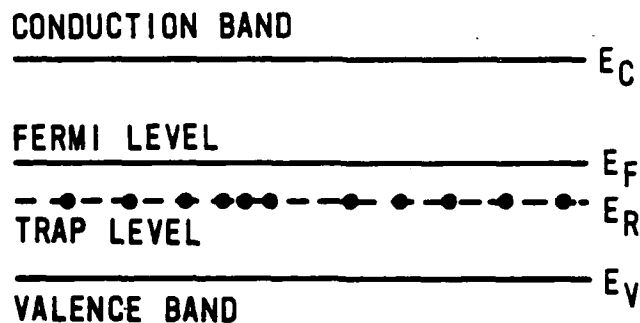
Figure 14. Energy band diagram for the case of injection with recombination centers partially filled.

Since trapped space charge exists, the neutrality approximation must be dropped and Poisson's equation now assumes the form

$$\left(\frac{k\epsilon}{e}\right)\left(\frac{dE}{dx}\right) = p + (p_R - p_{R.\omega}) - n \tag{121}$$

where $p_{R.\omega}$ is the empty recombination centers. In addition, the boundary conditions take the form $E = 0$ at $x = 0$ and $x = L$. The electron flow dominates at low current levels so that

$$J = e\mu_n \, nE \approx constant \tag{122}$$

and

$$\left(\frac{k\epsilon}{e}\right)\left(\frac{dE}{dx}\right) \approx p_R - p_{R..} \tag{123}$$

Since

$$\frac{n}{\tau_n} = \frac{p}{\tau_p} = \frac{n}{<v\sigma_n> p_R} = \frac{p}{<v\sigma_p> n_R} \tag{124}$$

then

$$p <v\sigma_p> n_R = n <v\sigma_n> p_R \tag{125}$$

Multiplying by e E and substituting from Equation 122 results in

$$J_p \approx \frac{\mu_p}{\mu_n} J_T \left(\frac{<v\sigma_n>}{<v\sigma_p>}\right)\left(\frac{p_R}{n_R}\right) \tag{126}$$

Since $p_R + n_R = N_R$ differentiating $\frac{p_R}{n_R}$ gives

$$\frac{d}{dx}\left(\frac{p_R}{n_R}\right) = \left(\frac{N_R}{n_R^2}\right)\frac{dp_R}{dx} \approx \left(\frac{k\epsilon}{e}\right)\frac{N_R}{n_R^2}\left(\frac{d^2E}{dx^2}\right) \tag{127}$$

Differentiating Equation 126 and substituting Equation 127 results in

$$\frac{dJ_p}{dx} \approx \left(\frac{k\epsilon\frac{\mu_p}{\mu_n}J_T <v\sigma_n> N_R}{e <v\sigma_p> n_R^2}\right)\frac{d^2E}{dx^2} \tag{128}$$

Simplifying gives

$$\frac{dJ_p}{dx} \approx -\left(\frac{J_T <v\sigma_n> p_R}{\mu_n E}\right) \tag{129}$$

This can be used in Equation 127 to obtain

$$E\left(\frac{d^2 E}{dx^2}\right) \approx -\frac{e <v\sigma_p> n_R^2 p_R}{ke\mu_p N_R} \approx -\frac{e <v\sigma_p> n_{R.o}^2 p_{R.o}}{ke\mu_p N_R} \tag{130}$$

This implies a threshold voltage independent of current level. Solving Equation 130 via simple approximations (from the low current conditions) yields,

$$V_{TH} \approx \left(\frac{e <v\sigma_p> L^4 n_{R.o}^2 p_{R.o}}{ke\mu_p N_R}\right)^{\frac{1}{2}} \tag{131}$$

a voltage barrier that must be overcome for the current to increase appreciably. Physically, this corresponds to a situation where the recombination centers must be filled to a major extent before current can flow--a trapped space charge must be overcome.

Further insight can be achieved through application of the Regional Approximation method, i.e., dividing the sample used into three sections. The third region in Fig. 15 corresponds to a region described by the most recent set of calculations, where Region III represents a potential barrier (i.e., V_{th} in Eq. 131) that must be dissipated. Local neutrality is assumed for Regions I and II. In Region I, $n(x) > n_{R,0}$ and the electrons are primarily in the conduction band; while in Region II, $n(x) < n_{R,0}$ and the population of the recombination centers is not changed from the thermal equilibrium values.

In Region I, $n(x) > n_{R..} p_R \approx N_R$. Local neutrality is detailed by

$$n - p = N_R - p_{R.o} = n_{R.o} \tag{132}$$

$$n = n_{p,o} \qquad n = \frac{ke}{e} \cdot \frac{de}{dk}$$
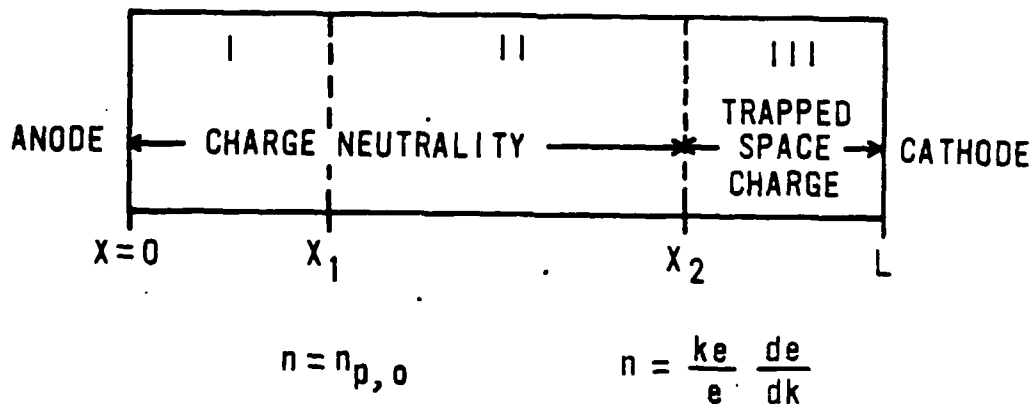
Figure 15. Schematic diagram of regions under consideration with boundary conditions.

47

Thus,

$$\frac{d}{dx}(n-p) = \frac{d}{dx}\left[(n_{R.o})E\right] = \frac{\left(\frac{\mu_p}{\mu_n}+1\right)\dot{n}}{\mu_p \tau_n} \tag{133}$$

and

$$\frac{1}{\tau_n} = <v\sigma_n> N_R$$

so

$$J_T = e\mu_n E(a+1)n - e\mu_p n_{R.o}E$$

$$a = \frac{\mu_p}{\mu_n} \tag{134a}$$

Letting

$$J_o = \left(\frac{J_T}{e\mu_p n_{R.o}}\right)$$

and

$$T = \frac{1}{\mu_n \tau_n} \tag{134b}$$

$$\left(\frac{E}{\frac{E}{E+J_o}}\right) dE = Tdx \tag{135}$$

the solution is

$$\ldots - J_o \ln\left[\frac{\cdots}{J} \quad J \quad \right] = Tx \tag{136}$$

Using the boundary conditions $E = 0$ at $x = 0$ results in

$$V(x) = \int_0^x Edx = \frac{1}{T}\left(\frac{1}{2}E^2 - J_o E + J_o^2 \ln\left[\frac{(E+J_o)}{J_o}\right]\right)$$

at

$$x = x_1$$

$$n_1 = n(x_1) = n_{R.o} \quad \text{and} \quad E_1 = E(x_1) = \left(\frac{J}{e\mu_n n_{R.o}}\right) = aJ_0 \tag{137}$$

and

$$x_1 = \left(\frac{J_0}{T}\right)(a - \ln(1+a))$$

$$V_{a.1} = \left(\frac{J_o^2}{T}\right)\left(\frac{1}{2}a^2 - a + \ln(1+a)\right) \tag{138}$$

48

as before, solving for J_m and V_m gives

$$J_m = h(a) \left(\frac{e n_{R.o} L}{\tau_n} \right)$$

and

$$V_m = \left(\frac{1}{g(a)} \right) \left(\frac{L^2}{\mu_n \tau_n} \right) \tag{139}$$

For $J \leq J_m$

$$x_1 = L \left(\frac{J_T}{J_m} \right)$$

and

$$V_{a.1} = V_m \left(\frac{J_T}{J_m} \right)^2 \tag{140}$$

For Region II, $n < n_R$, $n \ll n_{TR} - p_{R.o} \approx n \; n_R \approx n_{R.o}$. The neutrality and current conditions are

$$n = p_R - p_{R.o} = n_{R.o} - n_R \tag{141}$$

and

$$J_T = e \mu_n n E \tag{142}$$

Combining Equation 127 with Equation 141, and solving for the change of hole current with distance yields

$$\frac{dJ_p}{dx} = \frac{a J_T < v \sigma_n > N_R}{< v \sigma_p > n_R^2} \frac{dn}{dx} = -en < v \sigma_n > p_R \tag{143}$$

Substituting Equation 141 on the right-hand side (RHS), and n_R for $n_{R,o}$

$$-\frac{dn}{n(n + p_{R.o})} = \frac{e < v \sigma_p > n_R^2}{a J_T N_R} dx \approx \frac{e < v \sigma_p > n_{R.o}^2}{a J_T N_R} dx \tag{144}$$

since $dn = -\frac{J_T dE}{e \mu_n E^2}$ (from Equation 142) then

$$\frac{dE}{E - \left(\frac{J_1}{\mu_n E_R} \right)} = \frac{e < v \sigma_p > n_{R.o}^2 p_{R.o}}{a J_T N_R} dx \tag{145}$$

The point x_2 is where

$$n_2 = n(x_2) = \left(\frac{kt}{e} \right) \left(\frac{dE}{dx} \right)_2 \tag{146}$$

49

Mark and Lampert (Ref. 2) now change to the dimensionless variables

$$x = x^{\ddagger}w$$

$$E = E^{\ddagger}u$$

$$V = V^{\ddagger}v \tag{147}$$

$$X^{\ddagger} = \frac{aN_R J_T}{e<v\sigma_p> n_{R.o}^2 p_{R.o}}$$

$$E^{\ddagger} = \frac{aN_R J_T}{\{e<v\sigma_p> n_{R.o}^2 p_{R.o} k e \mu_p N_R\}^{\frac{1}{2}}} \tag{148}$$

$$V^{\ddagger} = \frac{(aN_R J_T)^2}{n_{R.o}^3 \{e<v\sigma_p> p_{R.o}\}^{\frac{3}{2}} \{ke\mu_p N_R\}^{\frac{1}{2}}} = E^{\ddagger}X^{\ddagger} \tag{149}$$

For Region I, Equation 134b becomes

$$\frac{udu}{u+c} = Ddw$$

$$C = \left(\frac{k\epsilon<v\sigma_p> p_{R.o}}{ea^2 \mu_p N_R}\right)^{\frac{1}{2}} \tag{150}$$

$$n = <v\sigma_n> N_R \left\{\frac{a^2 k\epsilon N_R}{e<v\sigma_p> n_{R.o}^2 p_{R.o}\mu_p}\right\}^{\frac{1}{2}} \tag{151}$$

solving Equation 150

$$U - C\ln\left[\left(\frac{U+C}{c}\right)\right] = Dw \tag{152}$$

for u = 0 at w = 0. For w corresponding to x, we find

$$w_1 = \left(\frac{C}{D}\right)(-a + \ln(1+a))$$

$$U_1 = aC \tag{153}$$

as in Equation 138. The dimensionless voltage $v_{a.1}$ is

$$v_{a.1} = \left(\frac{C^2}{D}\right)\left(\frac{1}{2}a^2 - a + \ln(1+a)\right) \tag{154}$$

For $w = w(L)$, Equation 153 and 154 can be rewritten as

$$w_c = \left(\frac{C}{D}\right)\left(a\left(\frac{u_c}{u_1}\right) - \ln\left(a\left(\frac{u_c}{u_1}\right) + 1\right)\right) \tag{155}$$

and

$$v_c = \left(\frac{C^2}{D}\right)\left(\frac{1}{2}a^2\left(\frac{u_c}{u_1}\right)^2 - a\left(\frac{u_c}{u_1}\right) + \ln\left(a\frac{u_c}{u_1 - 1}\right)\right) \tag{156}$$

For large injection levels, $u_c \ll u_1$, $w_c \approx \frac{u_c^2}{2CD}$, and $v_1 \approx \frac{u_c^3}{3CD}$. Therefore,

$$\left(\frac{v_c}{w_c^2}\right)^2 \approx \left(\frac{8}{9}\right) CD \left(\frac{1}{w_c}\right)$$

or

$$J_c \approx \frac{9}{8}e\mu_n n_{R.o}\tau_n \left(\frac{v^2}{C^3}\right) \tag{157}$$

which is the semiconductor injected plasma characteristic for $n_0 - p_0 = n_{R,0}$. Lampert and Mark go on to solve Regions II and III similarly to obtain the following equations for the current voltage characteristics.

$$\frac{1}{w_c} = \frac{aN_R}{e <v\sigma_p> n_{R.o}^2 p_{R.o}L}J_T \tag{158a}$$

$$\frac{v_c}{w_c^2} = \frac{1}{n_{R.o}L^2}\left\{\frac{ke\mu_p N_R}{ep_{R.o} <v\sigma_p>}\right\}^{\frac{1}{2}}V \tag{158b}$$

which are plotted in Fig. 16 for the following parameters: $\varepsilon/\varepsilon_0 = 12$, $\mu_n = \mu_p$ = 1 x 10^4cm^2/V-s, $n_{R.o} = p_{R.o}$ = 5 x 10^{14}cm^{-3}, $<v\sigma_n>$ = 10^{-9}cm^3/s and $<v\sigma_p>$ = 10^{-7}cm^3/s.

Figure 16 shows the general I-V characteristics for double injection in an insulator with partially filled recombination centers.

It should be noted that once the recombination centers are filled, the problem reduces to that of the trap-filled limit of the double-injection regime. Under actual conditions, the transition from single carrier-injection to double-carrier injection will depend on the rate at which voltage is applied to the speciman. Thus, the curve may be more rounded or abrupt in its transition to the $J \propto V^2$ regime.
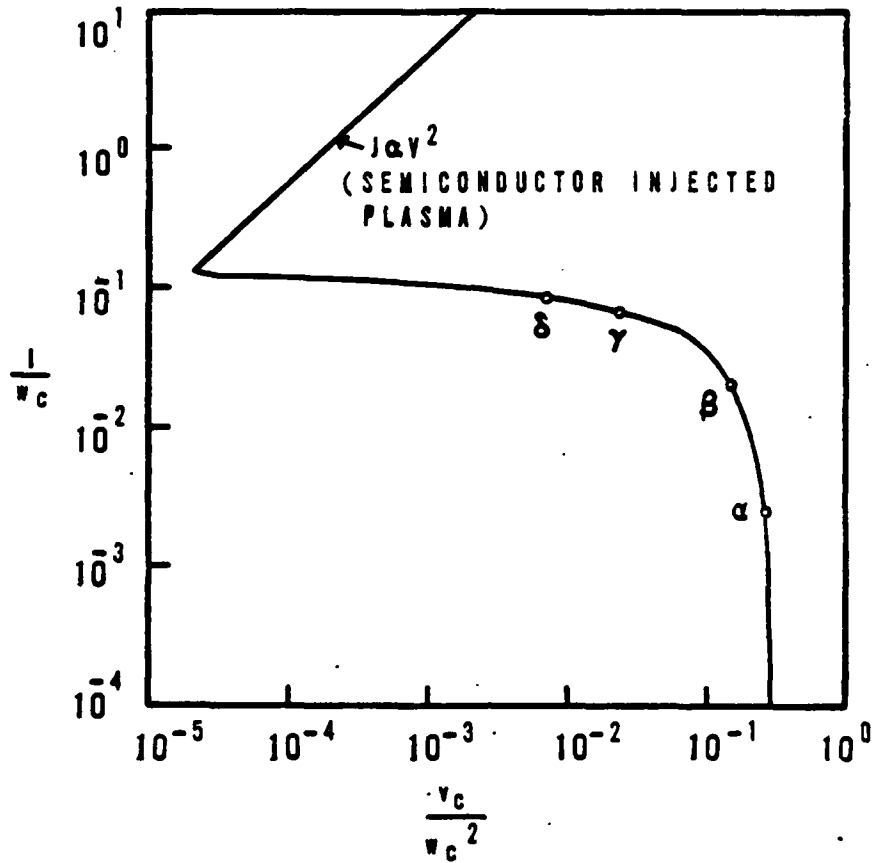
Figure 16.   General I-V characteristics for double injection in an insulator.

NOTE: The definitions of α, β, γ and δ on the curve are as follows: α--
Region I is 1 percent of the available volume, Region II is 1 percent of the
available volume, Region III is 97 percent of the available volume and 100
percent of Region V; β--Region I is 14 precent of the available volume,
Region II is 7 percent of the available volume, Region III is 79 percent of
the available volume and 100 percent of Region V; γ--Region I is 48 percent of
the available volume and 4 percent of Region V, Region II is 26 percent of the
available volume and 14 percent of Region V; and δ--Region I is 56 percent and
8 percent of V, Region II is 29 percent of the available and 35 percent of V,
Region III is 15 percent of the available volume and 59 percent of V.

DOUBLE INJECTION WITH TRAPPING-FREE THERMAL CARRIERS PRESENT

The same problem analyzed in the last section is now examined with a p-type insulator with thermal-free carriers (holes) present. The same assumptions apply as before except for the rewriting of Poisson's equation.

$$J_T = J = e\mu_n E + J = e\mu_p E = constant \tag{159}$$

$$\left(\frac{k\epsilon}{e}\right)\left(\frac{dE}{dx}\right) = (p - p_0) + (p_R - p_{R.o}) - n \tag{160}$$

$$\mu_n\left(\frac{d}{dx}\right)nE = -\mu_p\left(\frac{d}{dx}\right)pE = r - g \tag{161}$$

$$r - g = r_n = r_p - g_p \tag{162}$$

with $n_0 = 0$.

$$r_n = \frac{n}{\tau_n}$$

$$r_p = \frac{p}{\tau_p}$$

$$g_p = \frac{p_R}{\tau_r} \tag{163}$$

$$\frac{1}{\tau_n} = <v\sigma_n> p_R$$

$$\frac{1}{\tau_p} = <v\sigma_p> n_R$$

$$\frac{1}{\tau_R} = <ep> N_v \tag{164}$$

Trapped electrons are not allowed to be reemitted. Equation 159 becomes

$$J_T = J = e\mu_n E\left(1 + \frac{\mu_n}{\mu_p}\frac{p - p_0}{n}\right) + e\mu_p p_0 E \tag{165}$$

At this point, the quantity $(p - p_0)/n$ is assumed constant, independent of the injection level. This implies that

$$\frac{n}{\tau_n} = \frac{\frac{p-p_0}{n}}{\tau_p} \tag{166}$$

is true at low levels and high levels of injection. Thus,

$$\frac{1}{\tau_p} = <v\sigma_n> p_{R.o} = <v\sigma_p> n_{R.o} \tag{167}$$

and

$$\frac{\frac{p - p_0}{n}}{\tau_p} = \frac{\tau_p}{\tau_n} \tag{168}$$

Equation 165 now becomes

$$\mu_n \frac{d}{dx}(nE) = -\mu_p p_0 \left[1 + \underbrace{\frac{\mu_n}{\mu_p}\left(\frac{p - p_0}{n}\right)}\right]^{-1} \frac{dE}{dx} \tag{169}$$

Since free electrons are trapped quickly without reemission, the quantity underlined in Equation 169 must be quite small, resulting in

$$-\mu_p p_0 \frac{dE}{dx} \approx \frac{n}{\tau_n}\left(1 + \frac{p_R - p_{R,0}}{p_R}\right) \approx \frac{n}{\tau_n} \tag{170}$$

This equation can be rewritten in terms of the carrier transit time, using

$$t_p = \frac{k\epsilon}{ep_0\mu_p}$$

$$\tau_n = \frac{1}{<v\sigma_n> p_{R,0}} \tag{171}$$

Thus

$$\left(\frac{k\epsilon}{e}\right)\frac{dE}{dx} = -n\frac{t_p}{\tau_n} \tag{172}$$

$$J_T = e\mu_n nE - e\mu_p p_R E = constant \tag{173}$$

The last two equations are similar in form to those found in the one-carrier space-charge=limited current with shallow traps. The I-V relations can be written as

$$J = ep_0\mu_p\left(\frac{V}{L}\right) \tag{174}$$

where

$$V_z = \frac{L^2}{\mu_n \tau_n} \tag{175}$$

or the transit time equals the lifetime

$$t_n = \frac{L^2}{\mu_n V_z} \approx \tau_n \tag{176}$$

after which

54

$$J = \frac{9}{8} \left(\frac{\tau_n}{t_p} \right) k \epsilon \mu_n \left(\frac{V^2}{L^3} \right) \qquad (177)$$

When $t_p > \tau_n$, carriers are trapped, and the space-charge-limited current flow dominates. For $t_p > \tau_n$ double injection becomes prevalent.

Under realistic conditions, the assumptions above do not hold as well. The lifetime of carriers vary with injection level and captured carriers are reemitted. The net result is complicated equations which must be solved numerically.

If the variables are assumed to change slowly, the above equations still hold generally and the conclusion that as the lifetime and transit time became equal, double injection prevails over single carrier injection still holds.

This point is the one prevailing idea throughout the mathematical outline of double- and single-carrier injection. Thus, it is an important crossover point to understanding the conditions necessary for current filamentation.

CURRENT FILAMENT FORMATION

A notable aspect of the past mathematical treatment of various current flow problems is the appearance of current controlled negative resistance (CCNR) in I-V characteristics.

B. K. Ridley (Ref. 8) has pointed out that the occurrence of CCNR results in the formation of current filamentation. Therefore, the previous treatment provides clues to the initial conditions under which CCNR occurs.

To demonstrate the connection of the preceding sections to filament formation, Ridley's basic theory is examined in detail, bringing in concepts of the weakly or strongly ionized solid state plasma as they apply.

A bar of semiconductor material is subjected to a constant current and electric field and undergoes a perturbation under constant volume and pressure. The second law of thermodynamics as derived by Gibb (Ref. 9) is as follows

$$G \equiv U - TS + pV \tag{178}$$

where

G = Gibbs free energy

U = Total energy

T = Temperature

S = Entropy

P = Pressure

V = Volume

Under the second law, G is a minimum for a system in equilibrium. Thus, very little free energy exists in the system to drive instabilities or perturbations from equilibrium.

The Gibb's free energy is closely related to the helmholtz free energy allowing the statement of a thermodynamic identity relating the two.

$$dU = TdS - pdV + \mu d\rho \tag{179}$$

where

μ = total chemical potential

ρ = carrier density

Substitution of Equation 179 into the differential of Equation 178 under conditions described above and constant carrier density (or current) yields, dG = 0 and

$$TdS = dU - \mu d\rho \tag{180}$$

must be a minimum for a system in equilibrium.

Taking the time derivative of Equation 180 gives

$$T\frac{dS}{dt} = \frac{du}{dt} - \sum_k \mu_k \frac{d\rho_k}{dt} \tag{181}$$

where the last term is for all species of carriers (holes and electrons).

The application of an electric field results in a perturbation of the total energy and the chemical potential so that

$$\bar{U} = U + \sum_k e_k \rho_k \phi \tag{182}$$

$$\bar{\mu_k} = \mu_k + e_k \phi \tag{183}$$

where

e_k = charge per particle

φ = inner potential due to the applied field

The time derivative for Equation 167 is

$$\frac{d\bar{U}}{dt} = -div J_u + \sum_k e_k \rho_k \frac{d\phi}{dt} \tag{184}$$

where the total energy flow is J_u

$$J_u = J_q + \sum_k e_k J_k \phi \tag{185}$$

and J_q is the total heat flow. Under initial conditions the heat flow is equal to the electrical energy flow ($\sum_k e_k J_k \phi$). In addition, the continuity equation also holds.

$$\frac{d\rho_k}{dt} = -div J_k + \frac{\partial \rho_k}{\partial t} \tag{186}$$

57

Substitution into Equation 181 yields the following.

$$T\frac{dS}{dt} = \frac{d\bar{U}}{dt} - \sum_k \mu_k \frac{d\rho_k}{dt} \qquad (187)$$

$$T\frac{dS}{dt} = \left(-div J_u + \sum_k e_k \rho_k \frac{d\phi}{dt}\right) - \left(\sum_k \left((\mu_k + e_k\phi)\frac{d\rho_k}{dt}\right)\right) \qquad (188)$$

$$T\frac{dS}{dt} = \left[-div\left(J_q + \sum_k e_k J_k \phi\right) + \sum_k e_k \rho_k \frac{d\phi}{dt}\right]$$
$$- \left[\sum_k \mu_k \left(-div J_k + \frac{\partial \rho_k}{\partial t}\right) + \sum_k e_k \phi \left(-div J_k + \frac{\partial \rho_k}{\partial t}\right)\right] \qquad (189)$$

$$T\frac{dS}{dt} = \left[-div\left(J_q + \sum_k e_k J_k \phi\right)\right]$$
$$- \left[-\left(\sum_k \cdot \nabla\mu_k + \sum_k \nabla \cdot J_k\right) + \sum_k \mu_k \frac{\partial \rho_k}{\partial t}\right.$$
$$+ \left.\left(-\sum_k e_k J_k \cdot \nabla\phi - \sum_k e_k \phi \nabla \cdot J_k\right) + \sum_k e_k \phi \frac{\partial \rho_k}{\partial t}\right] \qquad (190)$$

using the following relationships

$$E = -grad\phi$$
$$J = \sum_k e_k J_k$$
$$J_q = -\sum_k e_k J_k \phi$$
$$\mu_k = -e_k\phi \qquad (191)$$

and

$$\sum_k e_k \frac{\partial \rho_k}{\partial t} = 0$$
$$\frac{\partial \phi}{\partial t} = 0$$

we find that

$$T\frac{dS}{dt} = -div\left(J_q - \sum_k \mu_k J_k\right) + \sum_k J_k grad\mu_k \frac{\partial \rho_k}{\partial t}$$
$$+ JE + \left(\sum_k (\mu_k + e_k\phi) div J_k\right) \qquad (192)$$

but

$$\sum_k (\mu_k + e_k\phi)div J_k$$

$$= div \sum_k \mu_k \dot{J}_k - \sum_k J_k grad\mu_k + div \sum_k e_k J_k \phi - \sum_k e_k J_k grad\phi$$

$$= grad(J_q - \sum_k J_k \mu_k) \tag{193}$$

where $grad = Tgrad\left(\frac{1}{T}\right)$ the temperature gradient

therefore

$$\frac{dS}{dt} = -div\left[\frac{J_q - \sum_k \mu_k J_k}{T}\right] + \frac{1}{T}\left[\left(J_q - {}_k J_k \mu_k\right) grad\right.$$

$$\left. + \sum_K J_k \, grad \, \mu_k - \sum_k \mu_k \frac{\partial c_k}{\partial t} + JE\right] \tag{194}$$

Which can be written as

$$\frac{dS}{dt} = -div J. + \frac{\partial S}{\partial t} \tag{195}$$

Where $J.$ is the entropy flow and $\frac{\partial S}{\partial t}$ is the entropy production rate. In the steady state, $\frac{dS}{dt}$ is zero as is $\frac{dU}{dt}$ and $\frac{c\rho_k}{dt}$. At equilibrium the production and flow of entropy is zero if the steady state is quite near equilibrium. Thus, $\frac{\partial S}{\partial t}$ should be as small as possible at equilibrium (i.e., minimal amount of free energy).

The concept invoked to justify the minimization of entropy production, namely, the principle of least entropy production, is acceptable as long as the definition of steady state is not synonymous with quasi-steady state. For this derivation, the time required to achieve the steady state must be very short compared to the duration of the experiment or observation.

If this is not the case then quasi-static situations prevail resulting in the production of entropy (or release of free energy) and ensuing instabilities in the solid state plasma formed (i.e., unstable electrical conditions as shown in the companion report).

Equation 194 can be applied to a semiconductor undergoing second breakdown and simplified if the temperature gradients in the material are assumed to be extremely small. Equation 194 simplifies to

59

$$\dot{s} = \sum_k \frac{grad\mu_k J_k}{T_k} + \sum_k \frac{J_k grad\mu_k}{Tk} + \frac{JE}{T} - \sum_k \frac{\mu_k}{T_k} \frac{\partial \rho_k}{\partial t} \tag{196}$$

Breaking Equation 196 down into the entropy production in the high current region ($\dot{s}_2$), and low current region ($\dot{s}_1$) upon filament formation, then

$$\dot{s} = \dot{s}_1(1-a) + \dot{s}_2 a + \lambda(\dot{s}_- + \dot{s}_+^-) \tag{197}$$

where a is the filament cross-sectional area (Fig. 17).

Two processes occur upon stabilization of the current filament: (1) the filament will grow or shrink depending on the amount of current shared in the low and high current regions and (2) the entropy production increases or decreases (increasing the circuit's entropy) for the semiconductor overall.

If stabilized, the temperature and chemical potential gradient will be zero and charge conservation will be observed. From symmetry, the terms in Equation 196 will cancel except JE/T. Thus, the only entropy source is that due to joule heating.

$$T\dot{s} = E_1 J_1(1-a) + E_2 J_2 a$$

$$J_0 = J_1(1-a) + J_2 a$$

$$T\dot{s} = EJ_0 = E(J_1(1-a) + J_2 a) \tag{198}$$

Then, the steady state is that in which the field E is a minimum or

$$a = \frac{J_0 - J_{10}}{J_{20} - J_{10}} \tag{199}$$

The cross-sectional area of the filament is in the same units used for the cross-sectional area of the sample. The build-up of a filament is inevitable upon examination of Poisson's equation

$$div E = \frac{4\pi}{\epsilon \epsilon_0} \sum_k e_k \rho_k \tag{200}$$

$$div \dot{E} = \frac{4\pi}{\epsilon \epsilon_0} - \sum_k e_k \dot{\rho}_k = \frac{4\pi}{\epsilon \epsilon_0} div J \tag{201}$$
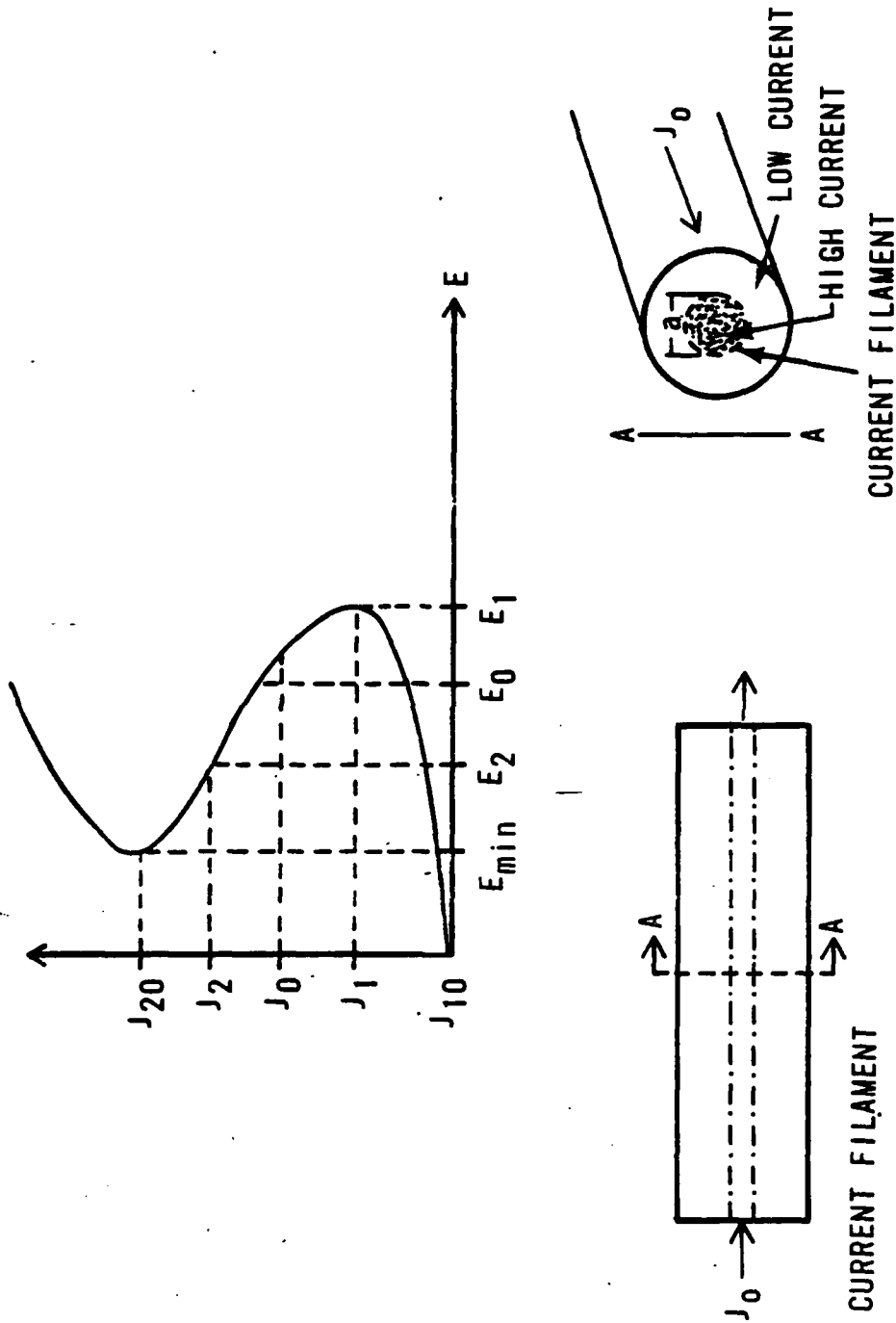
Figure 17. General J-V characteristics for differential negative resistance and idealized representation of a current filament.

Integration over the space-charge layers involved yields.

$$E_2 - E_0 = \frac{4\pi}{\epsilon\epsilon_0}(J_2 - J_0)$$ (202)

but

$$\triangle E_2 = E_2 - \bar{E}_0 = \frac{dE}{dJ}(J_2 - J_0) = \frac{dE}{dJ}\triangle J_2$$

then

$$\triangle \dot{J}_2 = -\frac{4\pi}{\epsilon\epsilon_0}\frac{dJ}{dE}\triangle J_2$$ (203)

and a negative differential resistance leads to the growth of the filament to a state where the minimum amount of entropy is produced under steady state conditions.

It should be noted that these derivations assume a zero phase difference between voltage and current, and a fixed total current. Dropping these assumptions adds two terms and a phase term to Equation 196. The added terms can result in driving forces that can feed instabilities (create free energy) and produce growing oscillations (Refs. 10, 11, and 12) that influence filament growth (Ref. 10).

Couched in terms of the previous derivation on carrier transport, the achievement of a transit time less than the lifetime creates an unstable electronic state that is mitigated by filament formation. This situation can become stable if all free energy (heating or external drive mechanisms) is removed from the device. If not, instabilities recurr resulting in an unstable plasma formation followed by thermal instabilities or growing oscillations.

APPLICATION TO GENERAL CASES

DEPLETION REGIONS AS INSULATORS AND SEMICONDUCTORS

As noted previously, the electrical characteristics of semiconductors are exploited by controlling the material's conductivity by passive (doping) and active (induced electric field) means. One way to unite passive and active modulation of conductivity is to form a metallurgic junction between dissimilarly doped materials. This type of junction is generally called a PN junction or diode (if p-type and n-type materials are joined). The materials reach equilibrium after joining to create a depletion region. So called because of the lack of mobile charge carriers.

The potential developed in the depletion region creates an electric field that sweeps the region free of mobile charges. Injecting a charge into the depletion region via regions adjacent to it demonstrates a distinctly different conductivity depending on the impressed electric field's polarity.

In forward bias, the depletion region exhibits a high conductivity similar to a heavily doped semiconductor. In reverse bias the depletion region exhibits low conductivity similar to an insulator (Fig. 18).

Basically, under low level conditions, the conductivity of a PN junction can be modulated over a wide range through variation of the strength or polarity of the applied electric field. Under high level conditions the conductivity is still modulated but is dependent on more than the electric field. New carrier transport mechanisms occur; nonlinearities due to carrier mobility changing with carrier energy occur, and variables become dependent on temperature and device architecture.

For example, the above PN junction can be driven into reverse bias by a strong electric field and initiate avalanche breakdown. The result is an increasing current capacity at a relatively constant voltage. The depletion region exhibits a constant or increasing conductivity in response to the applied voltage, similar to a metallic material.

By taking this type of approach to semiconductor transport problems the Regional Approximation Method becomes very useful in solving low and high level device characteristics.
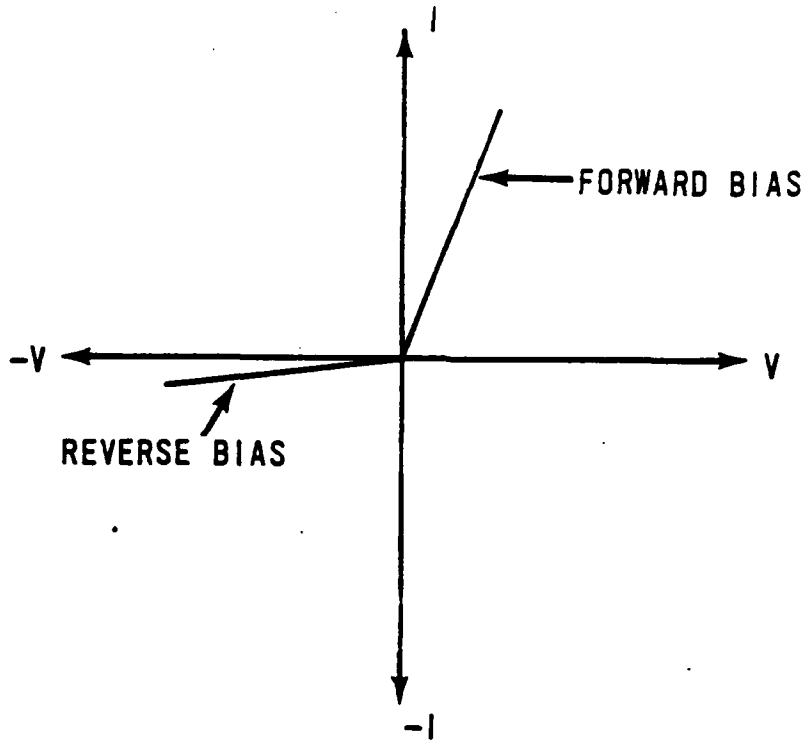
Figure 18.   Ideal low voltage I-V characteristics of
a PM junction.

PN JUNCTION--FORWARD BIAS

A demonstration of the utility of the Regional Approximation Method is easily performed for this case. An abrupt PN diode is detailed below for analysis ignoring thermal effects.

$P = N = 1 \times 10^{15}$ carriers/cm^3

total length = 2×10^{-1} cm

cylindrical geometry

radius = 5×10^{-2} cm

$\tau_n = \tau_p = 1 \times 10^{-6}$ s

$\mu_n = 1350$ cm^2/V-s

$\mu_p = 480$ cm^2/V-s

Built-in potential = 0.577 V

Unbiased depletion layer width = $1.7\,3 \times 10^{-4}$ cm

64

The diode is forward biased and passes a very small current on the order of the saturation current. The equations used to model behavior of a PN junction are well known and will not be derived here. By passing the low and moderate level injection regimes we now apply the Regional Approximation Method to the high level injection regime.

Under high level injection, the depletion region shrinks to a fraction of its original size. This follows from the application of an external potential which opposes and eventually counteracts the junction's built-in potential. As this occurs, the external potential begins to fall primarily on the bulk regions outside the depletion region.

As Fig. 19 shows, a potential gradient is impressed on these regions forming an electric field. Charge build-up near the contacts also contributes to an increasing electric field (Ref. 13).

Under low and moderate injection levels, the depletion region was the major influence on the devices characteristics. The situation changes dramatically under high level injection, bringing the bulk regions directly into play. With the depletion region's influence minimized, diffusion of carriers plays a very minor rule in controlling the device's characteristics. The electric field in the bulk regions initiates drift and space charge which allows a break-up of the device into two major regions where drift is dominant, and the recombination centers are full (ionized), as shown in Fig. 20.

The problem can be further simplified by examining one side of the diode, since the other side should react with the same transport properties.

Examination of the P of Fig. 20 side results in the formation of four zones in Region I (Fig. 21).

Electrons are injected from the cathode into the P region (Fig. 20) but cannot traverse the region completely before recombining. The transition region is required to smoothly join Region II with Region IV. This situation is exactly like the case of double injection with trapping (recombination centers are full--including space-charge effects). That is, a $J \alpha V^2$ followed by breakdown to another $J \alpha V^2$ regime. The Fig. 22 (from Ref. 14) shows the initial $J \alpha V^2$ does occur under appropriate conditions. The N-side can be drawn in the exact fashion as the in Fig. 21 as a mirror image (except for
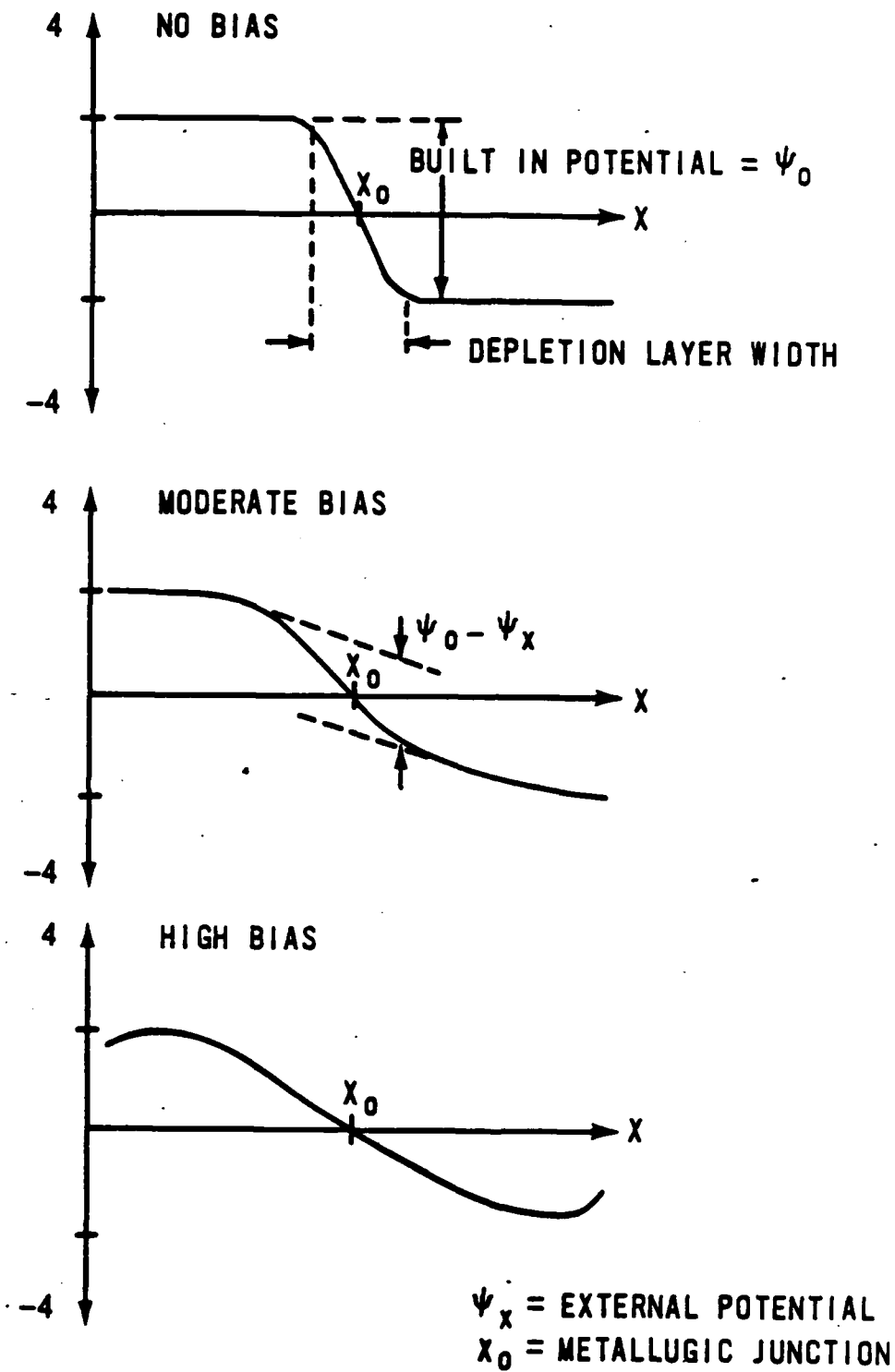
Figure 19. As the external potential increases and overcomes the built-in potential, the bulk regions become involved developing an electric drift field.

REMAINING
DEPLETION REGION

|←—REGION I—→|←—REGION II—→|

P   N

0   X_0 L
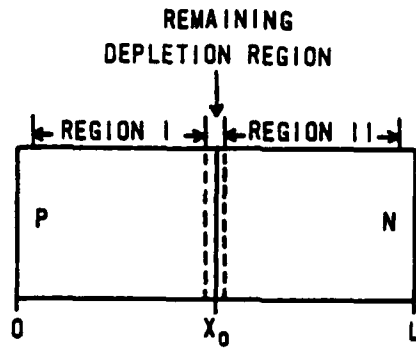
Figure 20.   Depiction of a PN junction under heavy forward bias (not to scale).

| I | II | III | IV |

NEGATIVE
SPACE
NEUTRALITY   TRANSITION   CHARGE
REGION   REGION   EDGE OF N
BUILD-UP   BULK REGION
ANODE   (CATHODE)

INJECTED
←—POSITIVE—→ $p<<n,(J \approx Jn)$
SPACE CHARGE

$X = 0$ X_1 X_2 X_3 $X_0 = 1/2 L$
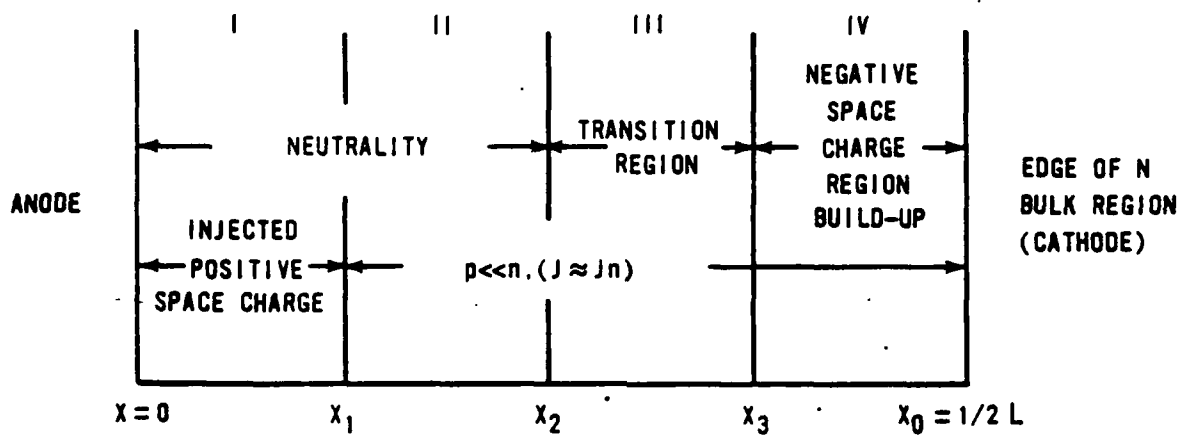
Figure 21.   Separation of the p-side into four regions similar to the double
injection with trapping case.
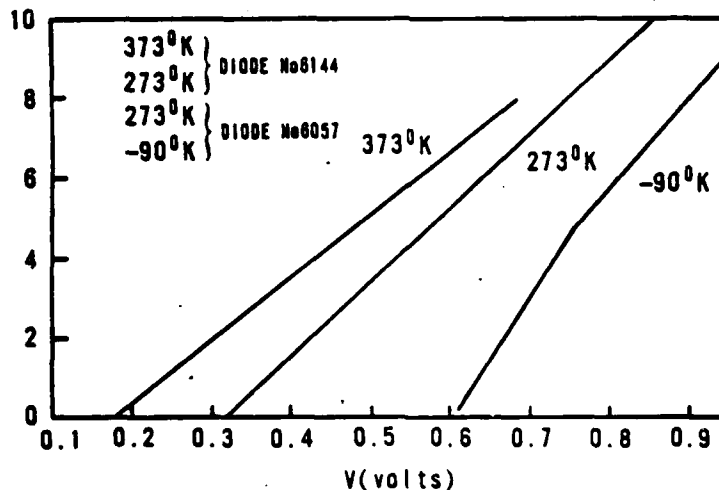
Figure 22.   Forward I-V characteristics for alloyed germanium diodes (Ref. 14).
The graph displays the $J \alpha V^2$ initial characteristic expected
before second breakdown.

the applied polarities). Solving one side of this problem for the general case provides a solution for the other side.

Page 34 provides the full problem description and general solution for this problem. The threshold voltage for breakdown is

$$V_{TH} = \frac{\mu_p L^2 N_R}{2\mu_p} = \frac{L^2}{2\mu_p \tau_p} \approx 10V \tag{204}$$

A smiliar expression holds for the N-side

$$V_{TH} = \frac{L^2}{2\mu_n \tau_n} \approx 7V \tag{205}$$

where L is the length of each bulk side, and V_{th} adds for the devices total potential difference.

The minimum voltage reached after breakdown is

$$V_m = \frac{1}{g(a)}\left(\frac{L^2}{\mu_p \tau_p}\right) + \left(\frac{L^2}{\mu_n \tau_n}\right)\frac{1}{g(a)} \tag{206}$$

with the associated minimum current density

$$J_m = h(a)\frac{e N_R L}{\tau_p} \tag{207}$$

As demonstrated by Equations 204 and 205, a situation arises where the transit time equals the lifetime of the carriers. Also known as

$$\text{transit time} \approx \text{Lifetime} = \frac{L^2}{V_{TH}\mu_p} \tag{208}$$

a transition from single carrier injection to double carrier injection. The ratio of these quantities yields the concept of gain.

$$\frac{J_{dblinj}}{J_{sglinj}} = \frac{\frac{Q}{t}}{\frac{Q}{\tau}} = \frac{\tau}{t} = gain \tag{209}$$

When t is equal to or less than τ the gain ≥ 1 and double injection dominates.

To solve for V_{th}, V_m and J_m for this diode we have a = 4 on the p-side and a = 4 on the n-side.

V_{th} (over total length) = 17 V

V_m (over total length) = 8.63 V

J_m (over total length) = 26.7 A/cm^2 ≈ 0.2 A

If thermal effects were allowed into the model, different results would certainly occur. Starting the simulation at room temperature would certainly ionize all impurities, while the electrical heating of the device would quickly make the material intrinsic and lower carrier mobility and decrease lifetime. This would decrease the value of V_{th}, V_m and J_m. A number of solutions are then possible dependent on the rate of heating and heat loss.

Use of Ridley's equations would yield the filament cross section near 60 percent of the device's area upon reaching Vm and Jm ignoring thermal effects. Adding thermal effects would no doubt increase the filament cross section.

Determining how the simulation would progress after filament formation with heating would quickly enter the realm of solid state plasma physics which is beyond the scope of this effort. The only definitive statement that can be made is sustaining operation after filament formation with heating will lead to device degradation via thermal shock.

PN JUNCTION--REVERSE BIAS

Under reverse bias, the diode considered here behaves quite differently. This analysis will concentrate on the aspects that occur after avalanche has begun.

The depletion region continues to grow as the applied potential increases. Thus, close attention will not have to be paid to the bulk regions. The depletion region has two distinct areas with different characteristics.

The avalanche region is basically neutral from the electron-hole pairs being created from impact ionization. The region involved in avalanche is less than one-tenth the length of the depletion region for a two-sided abrupt junction (Ref. 15) (Fig. 23). The remaining portion of the depletion region consists of traps that are partially filled. As carriers from the avalanche

AREA UNDER AVALANCHE

x_p 0 x_n

E

TO P BULK
REGION

TO N BULK
REGION

EMPTY NEGATIVE TRAPS   EMPTY POSITIVE TRAPS
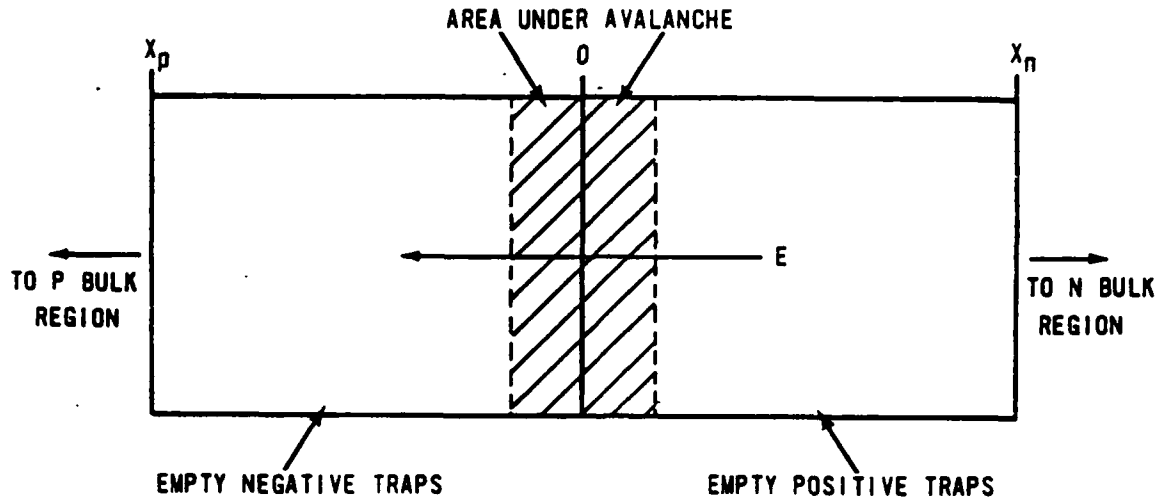
Figure 23.   Depiction of the depletion region of a reverse biased abrupt PN
junction. The shaded area is under avalanche injecting carriers
into the drift regions filled with traps (not to scale).

region enter the recombination zone space charge builds up from the inability
of the majority of carriers to transit as region without being trapped.

The injection from the bulk regions is very small and thermal excitation
is not adequate to relax the space charge. In addition, as the applied voltage
increases, the depletion region enlarges with the square root of the voltage.

The problem can be divided up as noted in Fig. 24. The region from $x = 0$
to x_1 is the avalanche region and is only a fraction of the width x. As the
applied voltage increases the fraction of x used by this region is still quite
small until very high fields (over 10^6 V/cm) are formed. The region from x_1
to x_2 is a transition region that varies in size dependent on the amount of
thermally excited carriers and the avalanche regions size. From x_2 to x_n the
trapped positive space charge dominates current flow. Basically, a recombina-
tion barrier exists that current flow (from $x = 0$ to x_n) must overcome. Single-
carrier injection is the prime mode of current flow.

Application of the Regional Approximation Method to this type of problem
was accomplished in solving the trap-filled limit problem (p. 9). The neutral
region expands with increasing voltage until the trapped space charge is over-
come, leading to double-carrier injection and CCNR.
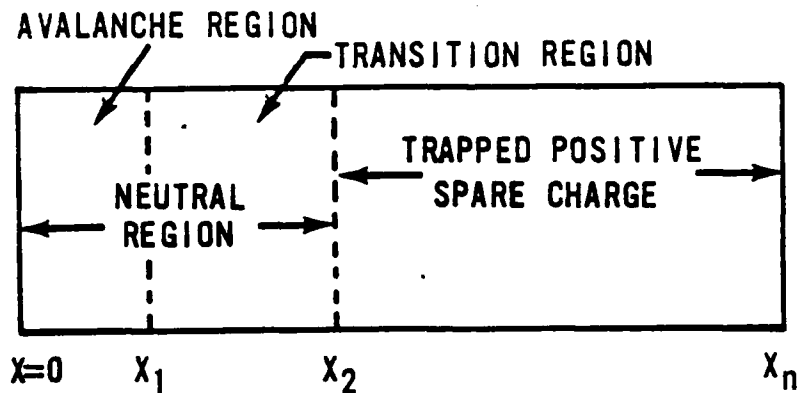
Figure 24. N side of the depletion region (not to scale).

All three regions expand with applied voltage, yet the neutral region will not expand to fill the space charge region until extremely high fields are attained. This is only probable for devices at liquid nitrogen temperatures where effects due to intrinsic carrier increases are minimal. At or near room temperature the increasing quantity of thermal carriers would be the primary cause of space charge relaxation leading to double injection (i.e., the point where the gain is greater than or equal to one).

Starting with the operating trap-filled-limit regime, a method of attachment must be developed which allows the use of changing lengths dimension and heating. An examination of p. 14 shows the critical current and voltage are

$$J_{cr} = \frac{2e^2 N_t \mu L}{k\epsilon} \quad \text{or} \quad V_{cr} = \frac{4e N_t L^2}{3k\epsilon} \tag{210}$$

for a crystal of length L. The depletion layer width, x_n, is defined in terms of the applied voltage as

$$x_n = \left(\frac{k\epsilon V_R (N_D + N_a)}{2e N_D N_a} \right)^{\frac{1}{2}} \tag{211}$$

where

$$\frac{N_D + N_a}{N_D N_a} = \frac{1}{N_t}$$

The equations noted in Equation 210 apply to the insulator part at the depletion region after avalanche occurs. This region occupies around 90 percent of the

depletion region. The voltage across x_n will be the voltage across the avalanche region and the voltage across the insulator.

The problem is simplified initially by ignoring thermal effects and holding the avalanche region at a constant length of 0.1 x_n, so that

$$\frac{0.1 x_n E_m}{2} = \psi_{\text{aval}} \tag{212}$$

where

Em = 2.25 x 10^5 V/cm

x_n = 1.4 x 10^{-3} cm

V_R = 337 V

From which we find ψ_{aval} = 16.65 v and the remaining potential drop across the insulator part of the depletion region is about 152 V. Solving for the voltage necessary from Equation 197, V_{cr} is about 362 V. To decrease the value of V_{cr}, L must be small compared to the avalanche region to overcome V_{cr}. Thus, $x_a \gg x_n - x_a$ before V_{cr} is achieved (for this particular example $x_a \sim .9 x_n$ before V_{cr} is overcome, thus thermal effects, are rejoined to aid the device).

If thermal effects are allowed in an isothermal situation, it is apparent that increasing intrinsic carrier concentration will lower N_t in Equation 210 by filling these traps. Thus, V_{ct} should become lower with higher temperature. The rate of heat absorbed and lost will determine when V_{cr} is lowered for a particular V_R.

This thermal assist mechanism can have a lesser effect if reemission of carriers is allowed in the insulator. Also, the addition of other impurities can affect lifetime and decrease or increase the chance for a thermal assist.

Solving these equations with all effects would require a great deal of knowledge about the semiconductor. Pertinent data left out of the equations can result in a large error. Effects due to very high fields such as changing mobilities, have not been considered and are beyond the scope of this report.

By examining the PN diode in forward and reverse bias the Regional Approximation method allows a definite insight to determine what precedes CCNR.

Both situations examined for a diode result in relaxation of an accumu-
lated space charge by increased single carrier injection. As single-carrier
injection dissipates the space charge, double-carrier injection follows with
CCNR and filament formation.

The particular examples studied here show thermal effects aid the elec-
tronic process by relaxing space charge build-up. Thus, the time history of
use and variables that effect the thermal characteristics of a device do play
a role in breakdown for these particular examples. Other device differences
(such as graded or exponential junctions) will require study on a case-by-case
basis to discern the transport mechanism but will still follow the same general
trends as these examples. .

It is important to note that thermal effects alone do not cause or initiate
the occurrence of CCNR. Thermal effects assist the initial conditions or relax
space charge, but it is the electronic transport, or transport gain that causes
CCNR and its accompanying effects.

PIN DIODE--FORWARD BIAS

This type of diode is used for high voltage applications primarily. The
extra I diffusion provides an additional expansion region for the depletion
region under high reverse and forward bias. The diode considered is detailed
below and in Fig. 25.

$P = N = 1 \times 10^{15}$ cm^{-3}, abrupt diffusions

I (n-type) $= 1 \times 10^{13}$ cm^{-3}

cylindrical geometry

radius $= 1 \times 10^{-2}$ cm

$\tau_n = \tau_p = 1 \times 10^{-6}$ s

$\mu_n = 1350$ cm^2/V-s

$\mu_p = 480$ cm^2/V-s

Built-in potential (PI junction) = 0.397 V

Unbiased depletion layer width (PI junction) = 7.19×10^{-4} cm

Built-in potential (IN junction) = 0.119 V

Unbiased depletion layer width = 3.94×10^{-4} cm
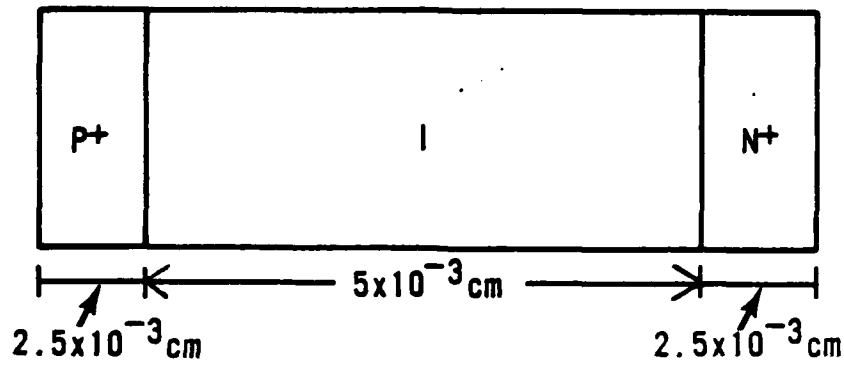
Figure 25.   PIN diode under consideration, not to scale.

Under high forward bias the depletion regions of a PIN diode will be reduced in size in a manner similar to a PN diode. The IN junction will be negated first by the applied voltage. The PI junction will eventually be negated, but not till a potential develops across the P and I regions. This potential gradient creates an electric field and the initiation of carrier drift. Holes are injected from the P region into the I region, while electrons are injected from the IN Junction. Region I is characterized as an insulator with fully ionized donor centers, which represent a recombination barrier to electrons.

Initially, the J-V characteristics will reflect a space charge limited current where $J \propto V^2$ (Ref. 2). As the current continues to increase, and direct recombination of carriers occurs the current transport characteristics transform to a semiconductor injected plasma. The J-V characteristics then conform to $J \propto V^2$ (Ref. 2) as noted in Fig. 13. As before, the threshold voltage is the same on a forward biased PN diode.

$$V_{TH} = \frac{L^2}{2\mu_n \tau_n}$$

where the average transit time equals the lifetime of electrons in the I region (the effects on forward voltage are seen in Ref. 16. For the PIN diode described, the V_{th} across the I region is about 9.2 mV. The voltage will drop at this point to about 4 mV across Region I while the current continues to increase. Heating rapidly destroys the device after CCNR occurs.

74

These effects assume that the lifetime and mobility (i.e., scattering mechanisms) are not altered by injection level, and space charge build-up is confined to very near the junctions. Under realistic conditions the relaxation of these requirements will increase V_{TH}.

PIN DIODE--REVERSE BIAS

Under reverse bias, the PIN diode resembles a long diode. At low and moderate voltages the diode exhibits a fairly low current $J \propto V$ tending toward $J \propto V^2$. The depletion region exists primarily in Region I, i.e., the insulator region. As the diode nears avalanche, the depletion region normally fills the insulator entirely. As avalanche occurs the entire insulator becomes filled with electron-hole pairs near the saturated drift velocity. Little of the depletion region extends into the P region and practically nothing extends into the N region.

If the avalanche coefficients are allowed to be equal, the avalanche breakdown voltage takes the form

$$V_{aval} = \frac{Wb}{\ln aW} \doteq 918 \ V \tag{213}$$

where

$b = 1.65 \times 10^6$ V/cm

$a = 1.6 \times 10^6$ V/cm

$w =$ insultator's width in cm

With an $E_{max} = 1.83 \times 10^6$ V/cm constant across the insulator. The electron-hole pairs produced in the insulator separate, holes leave the PI interface via diffusion and electrons leave the IN interface by diffusion. A small portion of the depletion region extends into the P region, but none penetrates the N region. Therefore, very few carriers trespass the junctions in large numbers since diffusion, not drift, dictates the current level.

The depletion region extends about 5×10^{-6} cm into the P region with a voltage drop of about 4.5 V. The only way to open the N junction for a large carrier flow is by increasing the potential till the N Junction reaches avalance allowing the space-charge accumulating in the insulator to relax (Fig. 26).
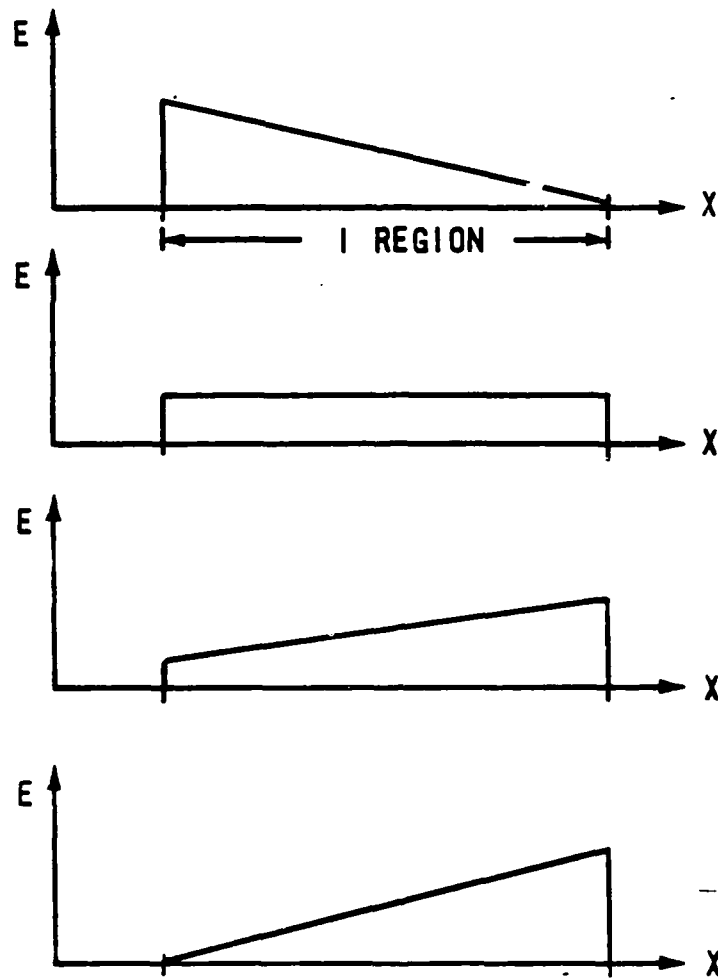
Figure 26. Change of the electric field with
position as the potential across
the device increases. The field
mimics the charge distribution
(not drawn to scale).

The distance the depletion region must penetrate into the P and N regions
must reach at least one debye length if avalanche is to be sustained (for the
avalanche multiplication to approach infinity).

The extrinsic debye length, L_D is

$$L_D = \left(\frac{k \epsilon V_T}{q |N_D - N_a|} \right)^{\frac{1}{2}} = 5 \times 10^{-5} \text{ cm} \tag{214}$$

To attain this distance on the N-side requires a potential drop of about 45 V. Thus the total voltage is 50 V (PI Junction) plus 918 V (for the insulator) and 45 V (at the IN junction) a total of 1013 V. At or near this voltage the N region junction will begin to avalanche injecting large numbers of carriers into the insulator and bulk regions passing a large current and reducing the insulators space-charge and field strength. The diode has transferred from single carrier injection dominated current flow (SCL current flow) to double-carrier injection in a trap-free insulator--also called the semiconductor $J \propto V^2$ regime. Filamentation follows the CCNR quite quickly. Experimental proof verifying the preceding description is given in Refs 15 and 17.

If thermal affects are allowed to enter into the situation several changes occur. Avalanche coefficients will decrease in magnitude due the phonon inter-action with free carriers. The intrinsic carrier concentration will increase rapidly (doubling for every 11 °C rise above room temperature) to effect the occupation of donor sites in the insulator. As the sites fill, the material becomes intrinsic decreasing the mobility and possibly changing the carrier lifetime. The increased carrier density in the bulk regions will encourage *farther diffusion and heighten the overall* current passed by the diode. To achieve avalanche in the bulk regions near the junctions will therefore require a higher potential. The voltage needed to breakdown the diode will therefore be higher.

The PIN diode shows many of the same conditions that precedes second breakdown in the PN diode. Under reverse bias, the initiation of conditions for second breakdown require avalanche breakdown in the bulk regions of the junctions. This is followed by space charge relaxation in the insulator and double injection.

BIPOLAR JUNCTION TRANSISTORS--SINGLE DIFFUSED

The Bipolar Junction Transistor (BJT) is the next step in the evaluation of diode technology. Today's BJTs are fabricated with many different types of diffusion processes and numerous architectures. Application of the Regional Approximation method to the transistor has been performed (Ref. 18) and will not be repeated here. Instead, the single diffused somewhat idealized transistor will be analyzed for special situations where large voltages are applied in various ways to achieve unstable device operation. This can then be

examined as special cases of unstable current states (CCNR) as shown for the PN and PIN diodes. Cases involving double-diffused BJT and field effect transistors will not be examined. The reader will find after some consideration that these devices are also special cases of the PN or PIN diodes.

The generic BJT examined here will not be quantified numerically with general mathematical criteria for unstable operation. The numerous types of BJTs and prolific architectures that are available often times dictate how the transistor parameters (α, β, spreading resistance etc.) are related at high bias. Therefore, general cases would have to be developed for each particular BJT type and architecture, which is beyond the scope of this report.

The device to be examined is a P-N-P single diffused BJT as shown in Fig. 27. Then, the BJT's most important dimension is base width and contact periphery. To achieve transistor action, the amplification of a signal, the emitter must be close enough to the collector to influence it. If the base is wide compared to the carrier diffusion length, excess carriers injected from the emitter cannot reach the collector and influence it. Therefore, the base width is on the order of a diffusion length. The base width directly influences a factor called the base transport factor, β. Beta represents the ratio of minority carrier current reaching the collector to the actual minority carrier current emitted. As such, it is also a measure of the carrier transit time divided by the lifetime. The value for β is usually slightly less than unity.

Another factor used to qualify the BJT is δ, the collector efficiency. This represents the ratio of collected to incident current on the collector and is normally less than unity. The final value of this variable is dependent on the value of the surface recombination rate.

The symbol γ is called the emitter injection efficiency and represents the ratio of minority current to total emitter current. The value of γ is normally less than unity.

All three factors listed above can be multiplied together to yield the factor α_B known as the current amplification factor. It is approximately equal to the negative of the total collector current minus the collector leakage current divided by the total emitter current.

$$\alpha_B = \beta\delta\gamma \approx -\left(\frac{I_c - I_{co}}{I_E}\right) \tag{215}$$

78

TRAPPED POSITIVE CHARGE

EMMITTER ○—— p++   n+   p+ ——○ COLLECTOR

BASE

TRAPPED NEGATIVE CHARGE
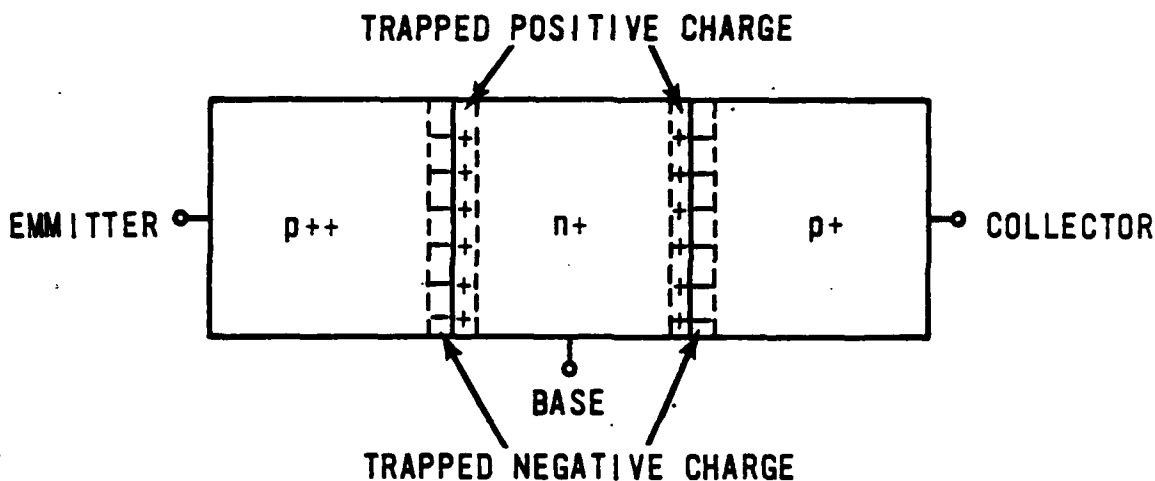
Figure 27.   Schematic diagram of a pnp transistor under no external bias (not drawn to scale). All junctions are abrupt diffusions.

Note that under any bias condition, either $(I_c - I_{co})$ or I_E will be negative by definition making α_B positive. Many aspects of transistor operation can be explained in terms of these variables including aspects of electronic instability in the four cases to be considered.

COLLECTOR BREAKDOWN

A p-n-p transistor is illustrated in Fig. 28 in the common base configuration

The first extreme of operation to be considered is avalanche breakdown of the collector junction with the emitter-base loop open. This is nothing more than simple diode breakdown already outlined in an earlier section.

In terms of the transistor variables outlined before, the actual number of minority carriers collected becomes much larger than the number of minority carriers that actually strikes the collector. This is, of course, due to avalanche breakdown of the collector.

Numerically, δ is determined by the multiplication coefficient of avalanche. This has been defined experimentally as

$$\delta = \frac{1}{1 - \left(\frac{V_{CB}}{BV_{CBO}}\right)^n}$$

$n = 2 \text{ to } 4$ (216)
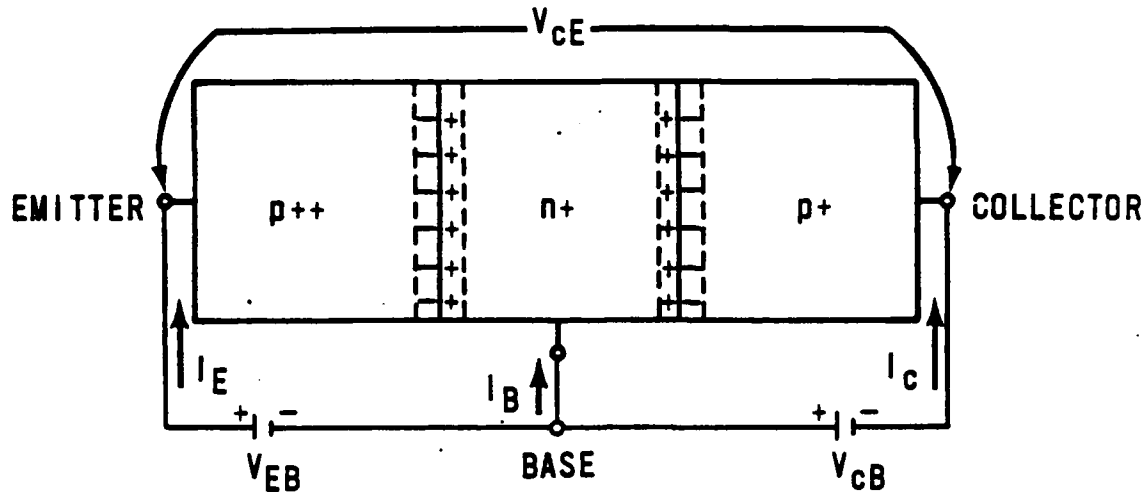
Figure 28.   A pnp transistor in the common base configuration.   The emitter is
forward biased with respect to the base.   The collector is reverse
biased with respect to the base.   Drawing is not to scale.

As δ tends toward infinity, so does α_B in Equation 215.   An electrical instabil-
ity will occur as described previously for the PN diode in reverse bias.   But,
two limitations apply specifically to transistors in this scenario.   The col-
lector depletion region cannot expand beyond the limit of the base region
without support of an external potential.   Since the base electrode is normally
located around the periphery of the base diffusion, the depletion region
expands preferentially toward those regions.   If the depletion region touches
the electrodes the space charge resistance (due to SCL current flow) will be
dissipated initiating double carrier injection.   The inclusion of surface
recombination or spreading resistance makes punch-through to an electrode much
harder.   Heating can bring the material into the intrinsic regime relaxing the
accumulated space charge and possibly initiating solid state plasma formation.

EMITTER--COLLECTOR BREAKDOWN

This situation is depicted in Fig. 29 with the emitter junction forward
biased and the collector junction reverse biased.   Initially, the base is to
be open.

Since the emitter is forward biased, there is a minority current into the
base.   If V_{CE} is greater then a few tenths of a volt, the emitter is injecting
a current into the base that is greater than the collector's reverse saturation
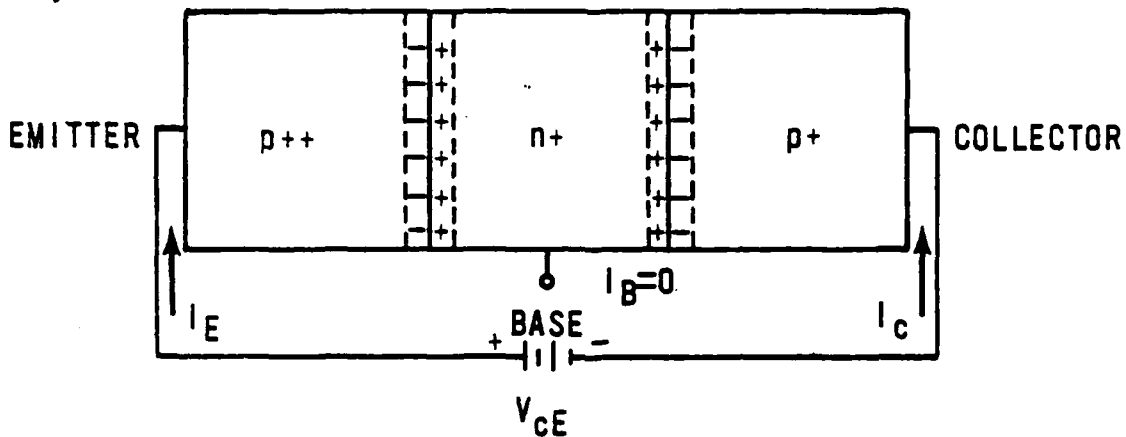
Figure 29. Set-up to study collector-emitter breakdown (not drawn to scale).

current. Thus, the current through the collector is larger than I_{CO}. This current is $\alpha_E I_E$ plus I_{CO} or I_{CEO}.

$$\alpha_E = \frac{\alpha_B}{1 - \alpha_B} \approx I_C \frac{1}{I_B}$$

$$I_{CEO} = I_{CBO}(1 - \alpha_E) \tag{217}$$

As V_{CE} increases, the width of the collector depletion region expands into the base increasing β and δ. V_{CE} also increases I_E and conversely γ. These increases boost α_B and I_C until avalanche is initiated. The increased quantity of carriers in the collector junction means avalanche is initiated at a lower field strength than BV_{CBO}.

Further increases in V_{CE} result in the collector depletion region reaching the emitter junction which provides carriers to relax the accumulated space charge initiating double injection and CCNR. This situation is quite similar to breakdown in a PIN diode.

In terms of the transistor variables, δ does not increase to infinity with higher V_{CE} until it is closer to avalanche. But β and γ increase to high values since

$$\alpha_E = \frac{\alpha_B}{1 - \alpha_B} \approx I_C \cdot \frac{1}{I_B} = \frac{\gamma\beta\delta}{1 - \gamma\beta\delta} \tag{218}$$

• The current I_C, rises dramatically. As punch-through occurs, the space charge relaxes, initiating double injection and CCNR (α_E will increase very rapidly as α_B increases to infinity with punch-through) as shown in the $I_C V_C$ plot of Fig. 30.

Now, allow the base to be connected back to the circuit in Fig. 29. The value I_B is not zero and is able to drain carriers out of the base. The immediate consequence of $I_B \neq 0$ is that I_{CEO} decreases from the last case dependent on the value of α_B at low level injection.

As V_{CE} is increased the last scenario is repeated with the following added complications. Since $I_B \neq 0$, current is flowing toward the periphery of the base to the electrical contacts. There is little resistance to carrier flow perpendicular to the junctions, but parallel flow meets considerable resistance because of the vector quality of carrier diffusion and drift in the base (Ref. 19). The exact amount of resistance is determined by the base width and overall geometry (Ref. 20). The net result of this spreading resistance is to make the center of the emitter less forward biased then the edges. Thus, current flow is higher at the edges than the center and the Early Effect serves to further enhance the overall potential build-up. The value of V_C will increase past BV_{CEO} until the potential across the accumulated space charge and spreading resistance is large enough to allow the carrier transit time to equal the carrier lifetime.

The resulting I_C versus V_C curve will behave as shown in Fig. 31. Curve B in Fig. 31 shows a CCNR aspect that results even if avalanche has already occurred at the collector junction. Such activity is specific to the BJT and is dependent on geometry and the external circuit. This type of activity has been demonstrated in Reference 21.

ELECTRICAL INSTABILITY DURING COMMON EMITTER MODE CUTOFF

The situations described previously cover most extreme forms of operations that can be discerned for a BJT used as a switch or amplifier. One case does remain where both emitter and collector are reverse biased simultaneously. This occurs when a BJT is used in the common emitter set-up shown in Fig. 32.

As V_{CE} and V_{EB} increase, the base becomes modulated by the expanding depletion regions. As the voltage reaches avalanche for both junctions the
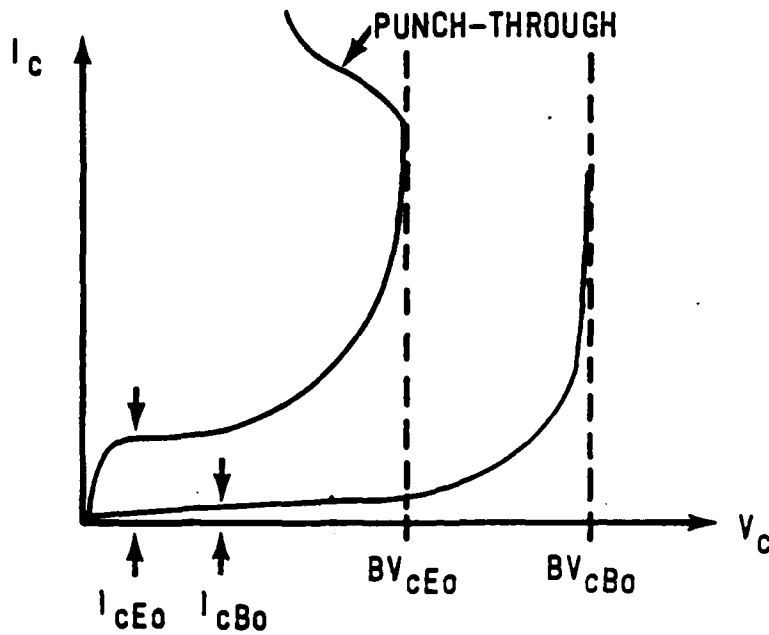
Figure 30. General I-V curves showing breakdown for
the collector-base compared to the col-
lector emitter breakdown (not to scale).
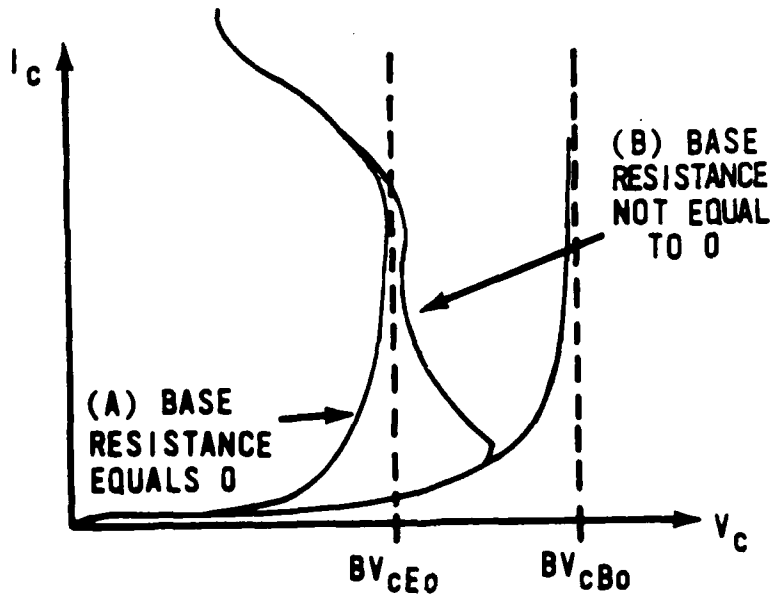
Figure 31. General I-V curves for collector-emitter
breakdown. Curve A is simple collector-
emitter avalanche breakdown with no
resistance in the base. Curve B is a
possible due to space charge build-up,
base spreading resistance, and some
external resistive ballasting (not to scale).

93
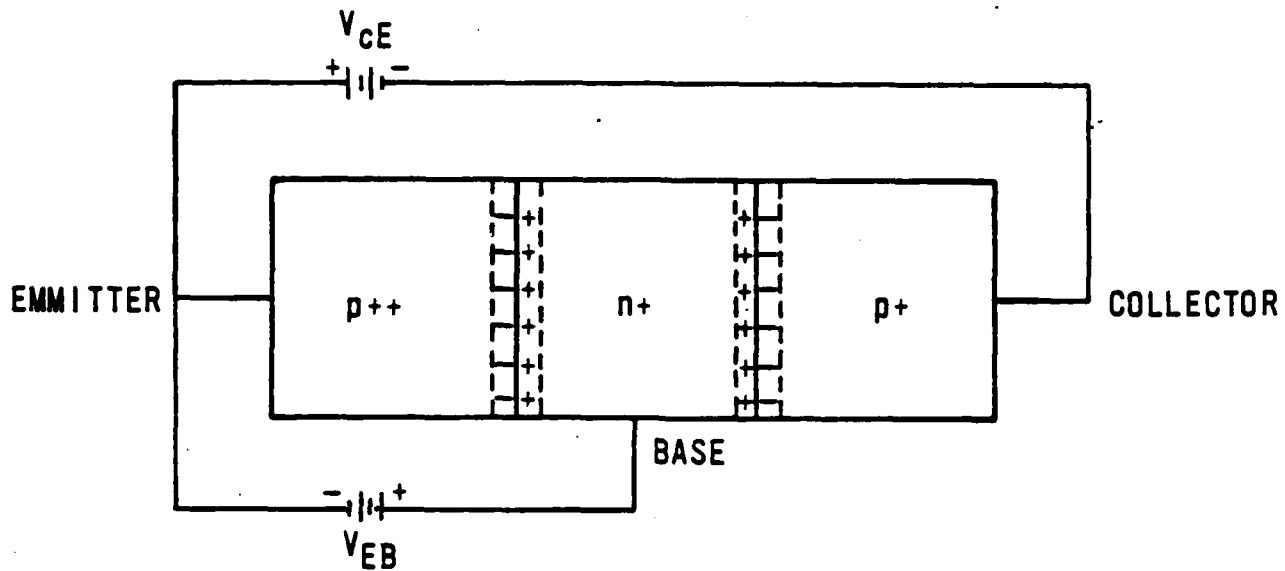
Figure 32. A pnp transistor in the common emitter setup (not to scale). Both junctions will be reverse biased to create a cutoff situation.

current injected into the base will be affected by base spreading resistance. This will reduce the potential near the center of each junction forcing current flow to the edges. The magnitude of this effect will be greatly dependent on geometry and the amount of current injected into the base. If the depletion regions expand into the base and merge we have the breakdown problem of the PIN diode. Space charge is relaxed and double carrier injection results. The I_C - V_C curve will behave as shown in Fig. 33.

For curve A, the base offers no resistance to current flow resulting in avalanche, punch-through, and double carrier injection. In terms of the transistor variables, α_E becomes very large and tends to infinity once punch-through occurs.

For curve B, spreading resistance due to the removal of carriers from the base results in an increase in V_C before avalanche can occur. This curve will also depend on the device geometry and external circuit. This effect may have been observed in Reference 21 numerous times. Also, curvature of the emitter-base deplet on region (due to the emitter area being smaller than the collector area) results in preferential avalanche near the regions of highest curvature while the collector-base junction will avalanche homogeneously. The
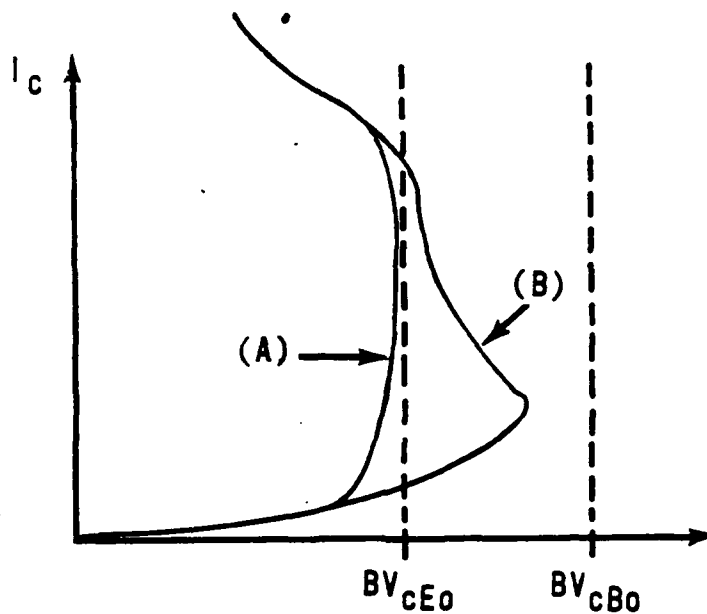
Figure 33. General I-V curves for breakdown
with the transistor in cutoff.
Curve A is for no resistance in
the base loop. Curve B is for
resistance in the base loop. The
amount of resistance will deter-
mine the shape of curve B (not
drawn to scale).

emitter-base avalanche is possibly current limited by surface recombination
and proximity to the base contacts. This will not allow β or γ to increase
with V_{EB}, and may very well decrease with increasing V_{EB}. It is even possible
that surface breakdown will limit V_{EB} before homogeneous avalanche can occur.

If the limitations of V_{EB} are ignored for now, the increased V_C values
needed before breakdown can occur are explainable by resistance effects.

CONCLUSIONS

The use of the Regional Approximation method allows in-depth analysis of devices under high level injection. Basic scenarios explaining how electronically unstable phenomena can occur have been detailed and applied to a simple PN and PIN diode. Application to transistors were detailed for cases of extreme operation.

An exhaustive application was not performed for all types of device diffusions, materials, or architectures. Instead, basic electronic transport problems in insulators and semiconductors was developed to show how injection level plays a significant role in determining J-V curves. These cases were shown to apply to device physics for a few major scenarios.

A vigorous connection was developed between the transition of single- to double-carrier injection and the initiation of current controlled negative resistance. This provides a basis for understanding the formation of current filamentation as a result of an electronically unstable situation.

Other methods of obtaining electronically unstable states relates to the quantum mechanical aspects of the material itself as elucidated in the companion report, "Analysis of Solid State Plasma Formation in Semiconductor Components," AFWL-TR-85-116.

REFERENCES

1. Kittel, C., Solid State Physics, Fifth edition, John Wiley and Sons, New York, New York, 1976, Chapters 7 and 8.

2. Lampert, M.A. and Mark, P., Current Injection in Solids, Academic Press, New York, 1970, Chapters 1, 2, and 14.

3. Bube, R.H., Electronic Properties of Crystalline Solids, Academic Press, New York, 1974, Chapters 5, 6, and 7.

4. Patrick, L., "Structure and Characteristics of Silicon Carbide Light-Emitting Junctions," Jour. of Appl. Phys. Vol. 28, No. 7, July 1957, p. 765.

5. Snyder, M.E., The Physics of Second Breakdown, AFWL-TR-83-22, Air Force Weapons Laboratory, Kirtland Air Force Base, NM, November 1983.

6. Mayer, J.W., et al., "Observation of Double Injection in Long Silicon P-I-N Structures," Phys. Ref., Vol. 137, No. 1A, Jun 1965, p. A286.

7. Marsh, et al, Appl. Phys. Letter 5, p. 74 (1965)

8. Ridley, B.K., "Specific Negative Resistance in Solids," Proc. Phys. Soc., Vol. 82, 1963, p. 954.

9. Chen, F.F., Introduction to Plasma Physics, Plenum Press, New York, 1977, pp. 184-197.

10. Harrison, M.J., "Collective Excitation of Degenrate Plasmas in Solids," J. Phys. Chem. Solids, Vol. 23, 1962, p. 1079.

11. Pines, D. and Schrieffer, J.R., "Collective Behavior in Solid State Plasmas," Phys. Ref., Vol. 124, No. 5, Dec 1961, p. 1387.

12. McKelvey, J.P., Solid State and Semiconductor Physics, Krieger Publishing Comp, Malobor, Florida, 1982, pp. 402-403.

13. Jonscher, A.K., "P-N Junctions at Very Low Temperatures," Brit. Jour. of Appl. Phys., Vol. 12, Aug 1961, p. 363.

14. Moll, J.L., Physics of Semiconductors, McGraw-Hill Book Comp., New York, New York, 1964, pp. 230-232.

15. Barnett, A.M. and Milnes, A.G., "Filamentary Injection in Semi-Insulating Silicon," Jour. of Appl. Phys., Vol. 37, No. 11, Oct 1960, p. 4215.

16. Choo, S.C., "Effect of Carrier Lifetime on the Forward Characteristics of High Power Devices," IEEE Trans. on Elec. Dev., Vol. ED-17, No. 9, September 1970, p. 647.

17. Holonyak, N., "Double Injection Diodes and Related DI Phenomena in Semiconductors," Proc. of the IRE, Vol. 50, December 1962, p. 2421.

REFERENCES (Concluded)

18. Willardson, R.K. and Beer, A.C., Semiconductors and Semimetals, Vol. 6, Injection Phenomena, Academic Press, New York, 1970, Chapter 1, pp. 87-96.

19. Gandhi, S.K., Semiconductor Power Devices, John Wiley and Sons, New York, New York, 1977, pp. 157-161.

20. Yang, E.S., Fundamentals of Semiconductor Devices, McGraw-Hill Book Comp., San Francisco, 1978, pp. 241-243.

21. Portnoy, W.M., Reverse Bias Second Breakdown in Power Switching Transistors, AFWL-TR-82-139, Air Force Weapons Laboratory, Kirtland Air Force Base, NM, May 1983.

END

7-87

DTIC